ANALYSIS OF FLAPPED RUDDER GAP EFFECTS

John G. Champlain

ANALYSIS OF FLAPPED RUDDER GAP EFFECTS

by

JOHN G. CHAMPLAIN

LIEUTENANT COMMANDER, U. S. NAVY

B.S., United States Naval Academy, Annapolis

(1961)

SUBMITTED IN PARTIAL FULFILLMENT OF THE

REQUIREMENTS FOR THE DEGREE OF

NAVAL ENGINEER AND THE DEGREE OF

MASTER OF SCIENCE IN NAVAL ARCHITECTURE AND

MARINE ENGINEERING

at the

MASSACHUSETTS INSTITUTE OF TECHNOLOGY

ANALYSIS OF FLAPPED RUDDER GAP EFFECTS

by

John G. Champlain

Submitted to the Department of Naval Architecture and Marine Engineering on May 14, 1971, in partial fulfillment of the requirements for the degree of Naval Engineer, and the degree of Master of Science in Naval Architecture and Marine Engineering.

ABSTRACT

A force and moment dynamometer was constructed to measure experimentally the effects of flap gap variation on the characteristics of an NACA Series 66 Modified airfoil section configured as a 30% flapped all movable rudder. The investigation revealed the effect on rudder characteristics of an open or closed gap and its width to be dependent upon the rudder's angle of attack and flap angle. Under certain circumstances an open gap is beneficial for performance and under others it is detrimental. Theoretical prediction of the open and closed gap lift coefficient for a 5 degree flap angle at a 10 degree angle of attack was verified except for its magnitude. The experimental value is significantly smaller than the theoretical value.

Thesis Supervisor: J. E. Kerwin

Title: Professor of Naval Architecture and Marine Engineering

ACKNOWLEDGEMENT

The author wishes to express his gratitude to Professor J. E. Kerwin, of the Department of Naval Architecture and Marine Engineering, who acted as thesis supervisor. His assistance and advice during the preparation of this thesis is greatly appreciated.

The assistance of S. D. Lewis, of the M.I.T. Marine Hydrodynamics Laboratory, during the design and experimental phases of this thesis is also most appreciated.

The author would also like to express his thanks to the San Francisco Foundation, and the Ship Research and Technical Division, Naval Ship Systems Command Headquarters for financial support. This assistance financed in part the construction cost of the dynamometer used in this investigation.

Table of Contents

List of Figures

I. INTRODUCTION

The concept of a flapped movable control surface is indeed the result of the realization that a change in the surface's geometry, namely, a change in camber, causes a change in the aerodynamic or hydrodynamic characteristics of the section. Flapped airfoils or high lift devices have been investigated extensively by aerodynamicists in search of a method to improve aircraft lift performance during take off and landing without effecting its high speed and cruising characteristics. The majority of information concerning lifting surfaces utilized in the field of naval architecture is closely associated to works in aerodynamics.

The most common type of hydrodynamic control surface is the all movable rudder, a symmetric section which develops its lift by variation in angle of attack. A second variation is a movable rudder positioned behind a fixed skeg which develops lift by the variation in camber. Thirdly is a combination of these types, an all movable rudder with a flap. This type of surface develops lift from both the angle of attack and camber variations. It is this type of control surface that the efforts of this thesis are mainly directed. The results will extend the experimental work conducted by Bottomley (2) and those experiments recently completed at the M.I.T. Marine Hydrodynamics Laboratory under the direction of Professor J. E. Kerwin.

Bottomley's results apply only to a skeg rudder with zero inflow angle. It was not until the most recent M.I.T. experiments conducted in 1970 that a family of flapped rudders was systematically tested to characterize the effects of flap angle deflection, angle of attack, ratio of flap area to total rudder area, percent of balance area to flap area, and inflow angle on lift, drag, rudder moments, and flap moments. As stated in reference (2) prior to 1965 there existed no theoretical method to predict such effects. In fact it was not until 1969 that a computerized method (13) was proposed that utilized theory described in references 3, 4, 10, 11, 12, and 14 to predict characteristics of flapped rudders.

The experiments conducted at M.I.T. involving an NACA 66 Modified section configured as a flapped rudder did not investigate the effects of gap width between the flap and the forward section of the rudder. Reference 13 describes a theory which predicts the effects of gap width for a rudder of the 66 series for a particular flap angle at a particular angle of attack.

In order to analyze the theoretical predictions and further the effort to develop substantial experimental results, this thesis investigates experimentally the effects of gap variation on a 30% flapped rudder of a section similar to those rudders previously tested at the M.I.T. Marine Hydrodynamics Laboratory and considered in reference 13.

As with most devices there exists a limitation on the use of a flapped all movable control surface. Generally, if size is a controlling criterion of design, or the performance in astern operation is not critical such a surface is adequate. A fin stabilizer on commercial and naval vessels, and flapped keels on sailing yachts are examples of proper use of such a control surface. The fact that a 30% flapped control surface is representative of the type which is used for both purposes dictated the choice of such a rudder as the subject of this investigation.

The motivation for the work of this thesis stems from the fact that information in this area of naval architecture is minimal, and that until thorough complimentary experimental and theoretical analysis is conducted, proper selection of an optimum rudder for specific control requirements is not possible.

II. PROCEDURE

The Model

The model used in this investigation is a NACA series 66 Modified airfoil section configured as an all movable type of flapped rudder. The flap is an unbalanced type with a surface area total rudder area ratio of 0.30. The model is a cast bronze construction, with a rudder hinge line 2.917 inches from the root section leading edge, and a flap hinge line 6.417 inches from the leading edge. More detailed specifications and dimensions are contained in figure 1. Variation of the flap hinge line postion and therefore the gap width, the distance between the forward section trailing edge and the flap section leading edge, is accomplished by positioning the adjustable tip and root flap hinge brackets.

Tunnel Wall Corrections

The tunnel wall interference corrections developed in reference 5 modify the angle of incidence of flow and the drag coefficient. These coefficients are:

$$\text{Angle Correction} = 0.137(S/C)*C_L$$

$$\text{Drag Coefficient Correction} = 0.137*(S/C)*C_L^2$$

Figure 1

Model Specifications and Dimensions

Taper Ratio 0.60
Geometric Aspect Ratio 1.40
Root section Thickness Ratio 0.20
Tip section Thickness Ratio 0.10
Length 10 inches
Sweep of quarter chord 11 degrees aft
Mean Chord 7.142 inches

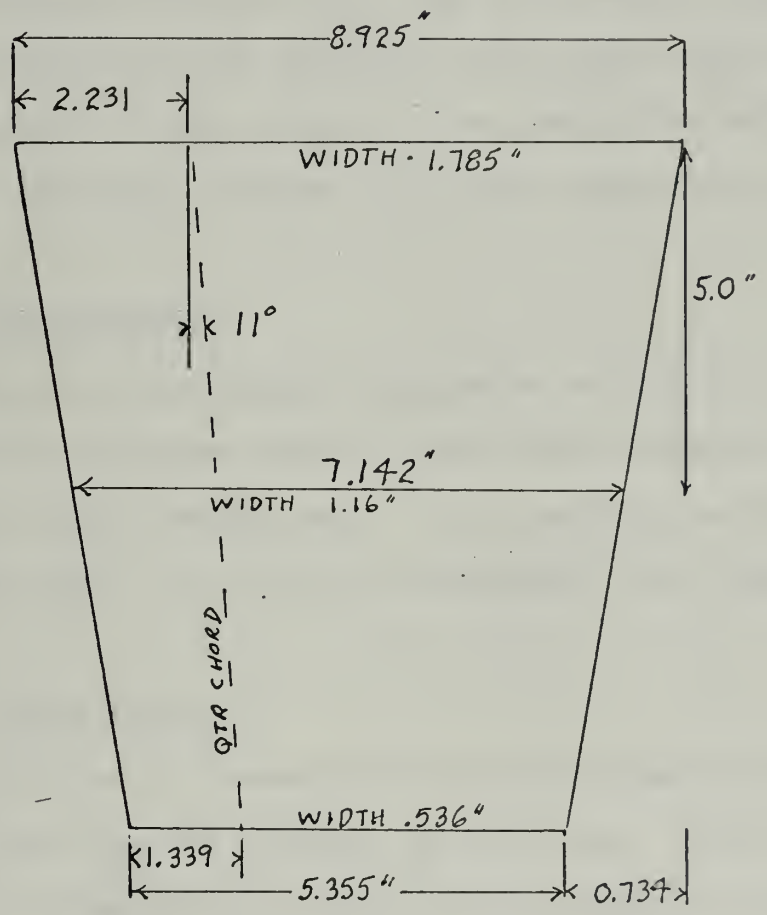

Test Procedure

The variable speed, variable pressure water tunnel of the Department of Naval Architecture and Marine Engineering was utilized for the tests. The rudder was tested in two modes at three flap gap width settings, 0.020, 0.050, and 0.100 inches. Mode One tests are conducted with the gap open, and Mode Two tests with the gap closed and faired. The material used to fair the flap gap is modeling clay of the quality associated with aircraft wind tunnel experimentation. This type of clay proved to be compatible with the environment of the water tunnel. The test procedure is as follows:

1. Gap Width Setting

This is accomplished by placing the proper amount of shim stock between the trailing edge of the rudder forward section and the flap leading edge. This setting is fixed by the friction type root and tip adjustable flap hinge brackets.

2. Flap Angle Setting

The flap angle is set by means of a friction clamp located at the root hinge bearing surface of the flap. The angle measurement is determined by a flap angle template incremented at 5 degree intervals.

3. Mounting Model/Position Fairing Plate

The model position in the dynamometer is fixed by a keyed friction clamp secured to the rudder shaft and the dynamometer spider. In order to reduce cross flow at the rudder root, a fairing cover plate is installed on the dynamometer window over the rudder root hinge bracket recess.

4. Set Load Cell Indicators

The rudder-dynamometer unit is mounted in the water tunnel and the tunnel is filled in preparation for the tests. Zero settings are then set on the load cell digital indicators. The indicators were previously calibrated with the standard calibrate resistors. The indicator zero settings are as follows: station one, 100 counts; station two, 50 counts; station three, 50 counts; station four, 100 counts; and station six, 50 counts.

5. Conduct Test

The operational test consists of measuring the angle of zero normal force followed by recording all load cell indicator readings resulting from a dynamometer angle variation from + 30 degrees to - 30 degrees in increments of 5 degrees. The water speed is maintained at 20 fps for the entire test period. Following this routine the load cell zero readings are recorded.

6. Flap Angle Variation

Steps 2 through 5 of the test procedure are repeated for each flap angle. The flap angle variation is 0 to 35 degrees in 5 degree increments.

7. Change of Mode

The entire procedure is repeated in Mode Two with the flap gap faired with modeling clay.

8. Change of Gap Setting

After the rudder is tested in both Mode One and Mode Two at a desired gap width setting, steps 1 through 7 are conducted at a new flap gap setting.

9. Data Reduction and Graphical Representation

The data is recorded on IBM Fortran sheets in a format compatible with that described in the Data Reduction Computer Program and reduced to coefficient form. The output of the data reduction program is plotted by a computer controlled plotter.

III RESULTS

The experimental results are represented graphically by figures 2 through 26.

Figure 26 compares the theoretical predictions (13) of the lift coefficient variation with gap width with the experimental values. This comparison is at a flap angle of 5 degrees at a 10 degree angle of attack.

The variation of lift coefficient with angle of attack and flap angle for each gap width investigated appears in figures 2 through 7. Figures 8 through 13 illustrate the effects of gap width variation on drag coefficient. Rudder moment coefficient variations are described by figures 14 through 19, and changes in center of pressure coefficient for both lift and drag forces are illustrated in figures 20 through 25. The forces and moments were non-dimensionalized according to expressions found in the Data Reduction Program.

The model at zero flap angle contained slight imperfections of symmetry caused by two sources; the model casting and the inability to set the flap at zero flap angle with precision. It must be emphasized that this imperfection in symmetry at zero angle is minute and within the bounds of normal engineering testing tolerance when the cost involved to develop a precision casting and a precision flap positioning mechanism is considered.

The slight shift of the original lift and drag data was caused by this symmetry imperfection. This was removed by a simple shift routine in the curve plotting computer program.

Figure 2

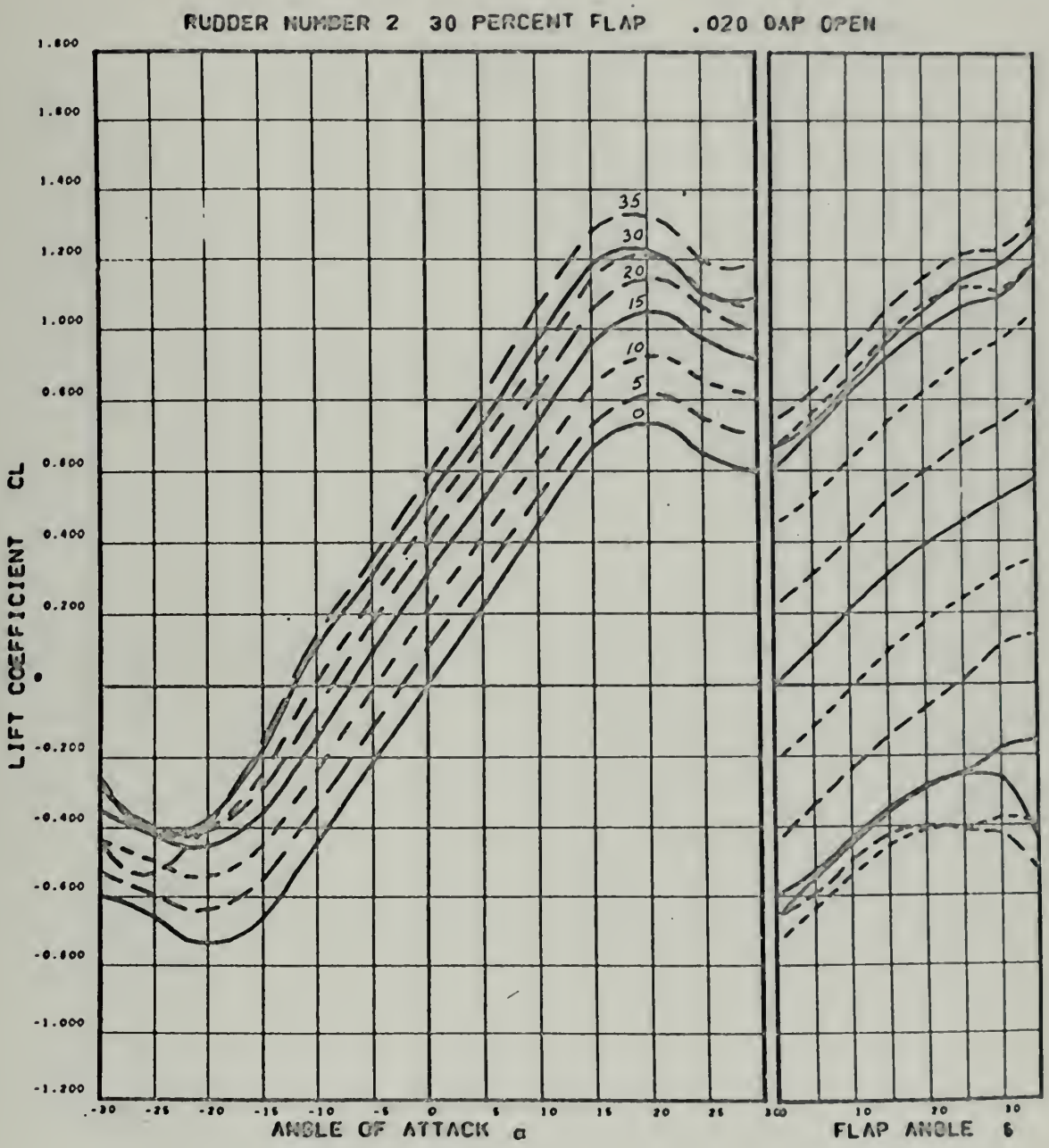
RUDDER NUMBER 2 30 PERCENT FLAP .020 GAP OPEN
LIFT COEFFICIENT CL
1.800
1.600
1.400
1.200
1.000
0.800
0.600
0.400
0.200
-0.200
-0.400
-0.600
-0.800
-1.000
-1.200
35
30
20
15
10
5
0
-30 -25 -20 -15 -10 -5 0 5 10 15 20 25 30
ANGLE OF ATTACK α
10 20 30
FLAP ANGLE δ

Figure 3

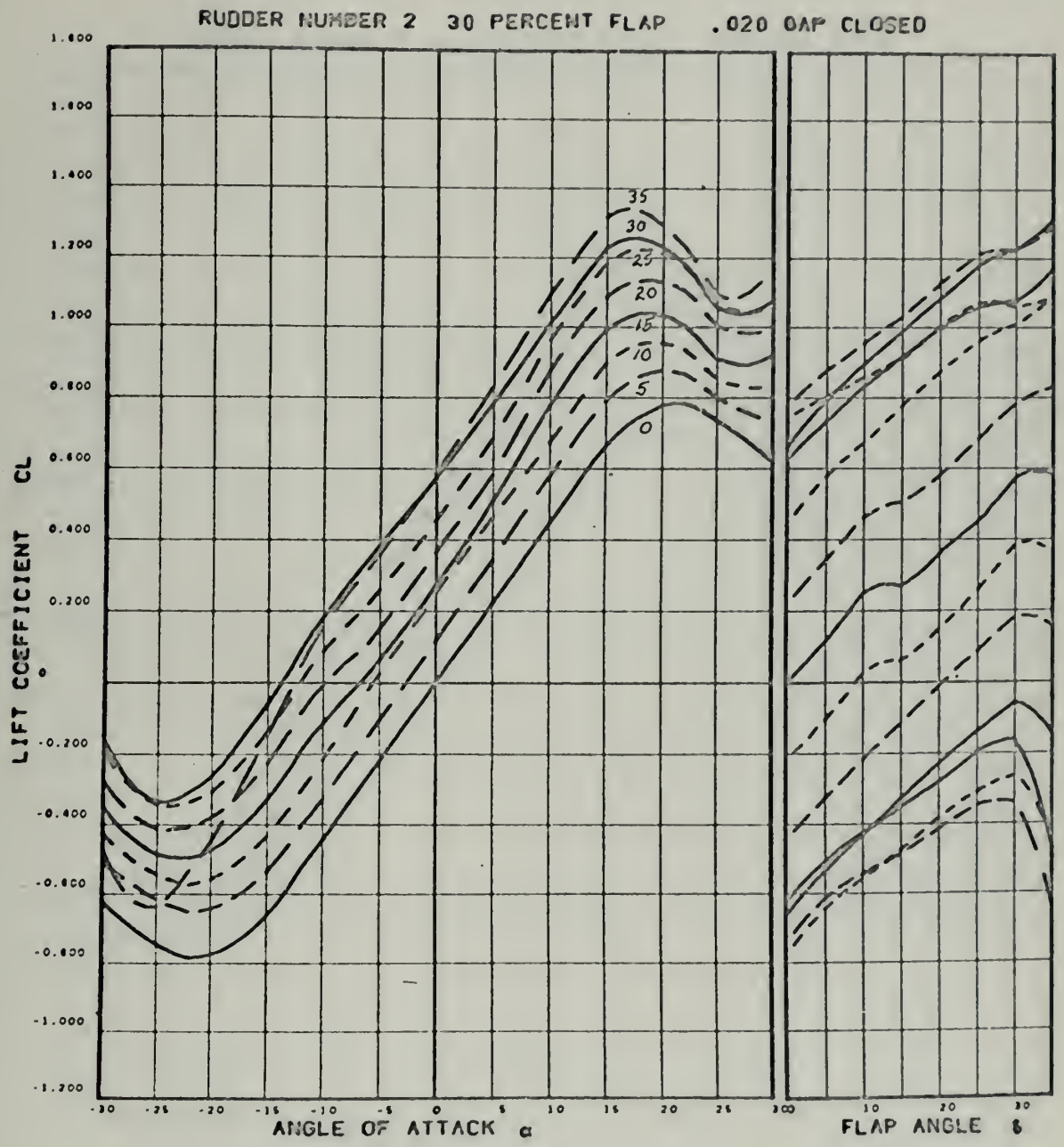
RUDDER NUMBER 2 30 PERCENT FLAP .020 GAP CLOSED
LIFT COEFFICIENT CL
1.600
1.800
1.400
1.200
1.000
0.800
0.600
0.400
0.200
0
-0.200
-0.400
-0.600
-0.800
-1.000
-1.200
35
30
25
20
15
10
5
0
-30 -25 -20 -15 -10 -5 0 5 10 15 20 25 30
ANGLE OF ATTACK α
10 20 30
FLAP ANGLE δ

Figure 4

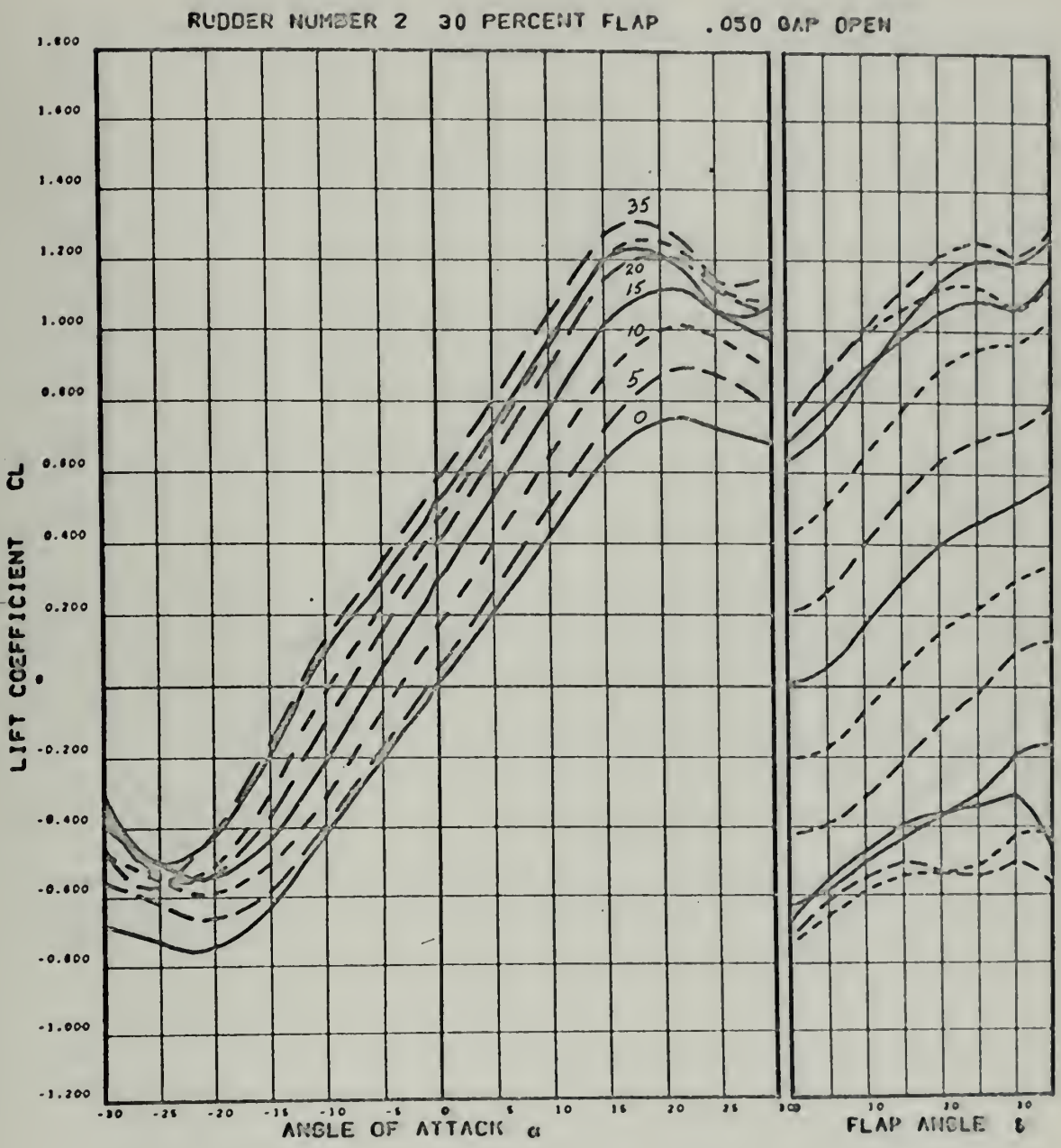
RUDDER NUMBER 2 30 PERCENT FLAP .050 GAP OPEN
LIFT COEFFICIENT CL
1.800
1.600
1.400
1.200
1.000
0.800
0.600
0.400
0.200
-0.200
-0.400
-0.600
-0.800
-1.000
-1.200
35
20
15
10
5
0
-30 -25 -20 -15 -10 -5 0 5 10 15 20 25 30
ANGLE OF ATTACK α
10 20 30
FLAP ANGLE δ

Figure 5

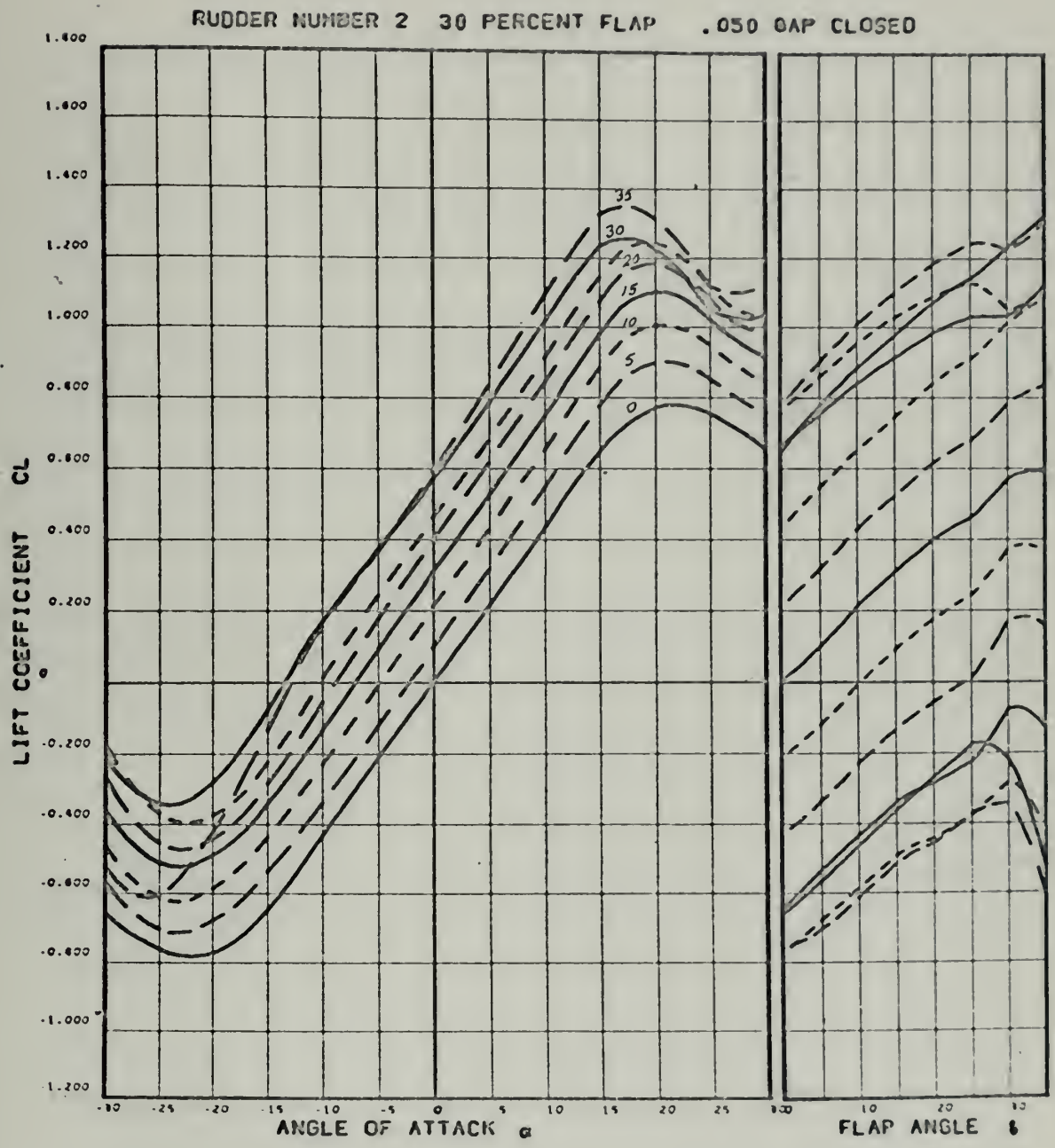
RUDDER NUMBER 2 30 PERCENT FLAP .050 GAP CLOSED
LIFT COEFFICIENT CL
1.400
1.600
1.400
1.200
1.000
0.800
0.600
0.400
0.200
0
-0.200
-0.400
-0.600
-0.800
-1.000
-1.200
35
30
25
15
10
5
0
-30 -25 -20 -15 -10 -5 0 5 10 15 20 25 30
ANGLE OF ATTACK α
10 20 30
FLAP ANGLE δ

Figure 6

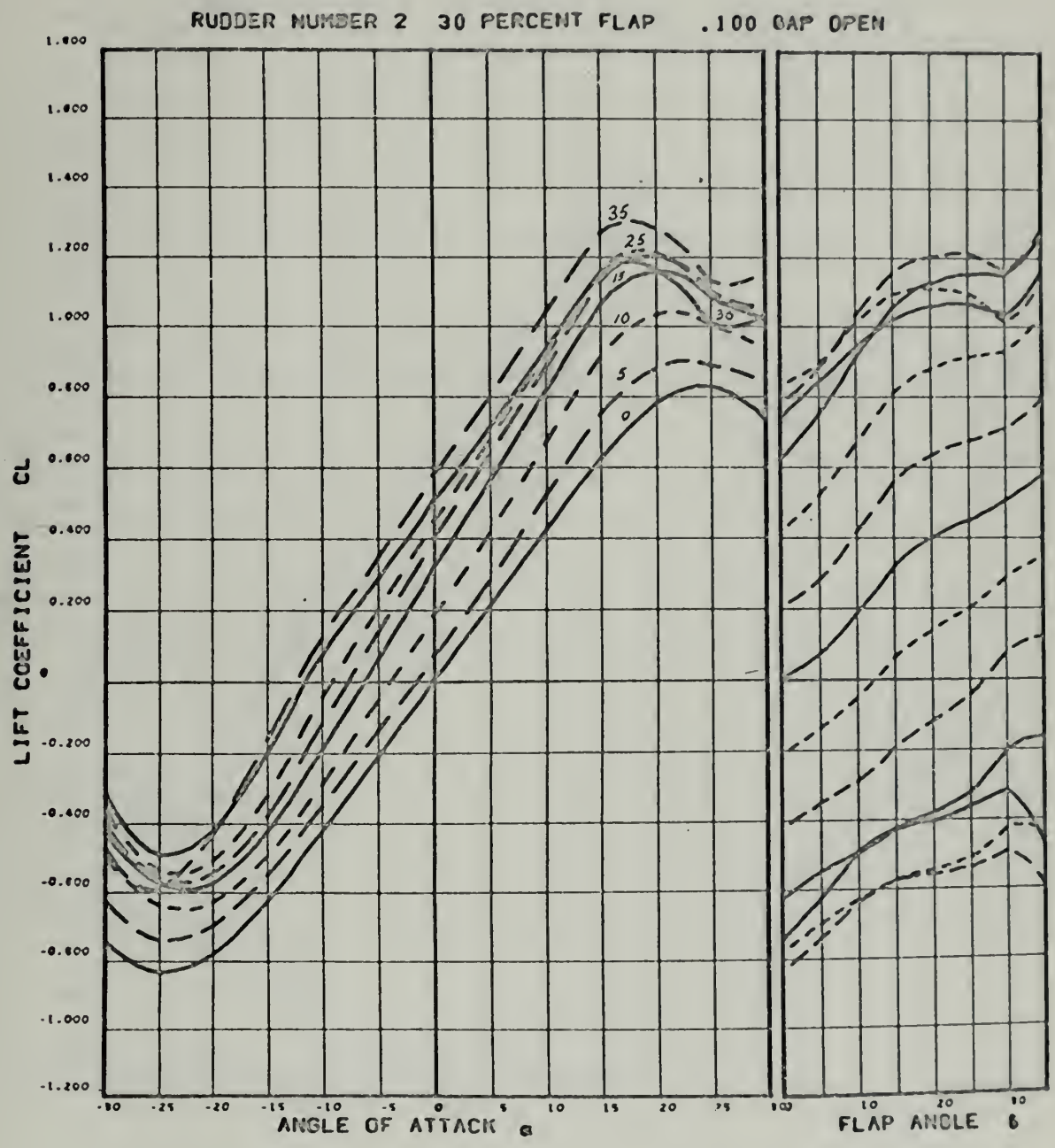
RUDDER NUMBER 2 30 PERCENT FLAP .100 GAP OPEN
LIFT COEFFICIENT CL
1.600
1.800
1.400
1.200
1.000
0.800
0.600
0.400
0.200
-0.200
-0.400
-0.600
-0.800
-1.000
-1.200
35
25
15
10
5
0
30
-30 -25 -20 -15 -10 -5 0 5 10 15 20 25 30
ANGLE OF ATTACK α
10 20 30
FLAP ANGLE δ

Figure 7

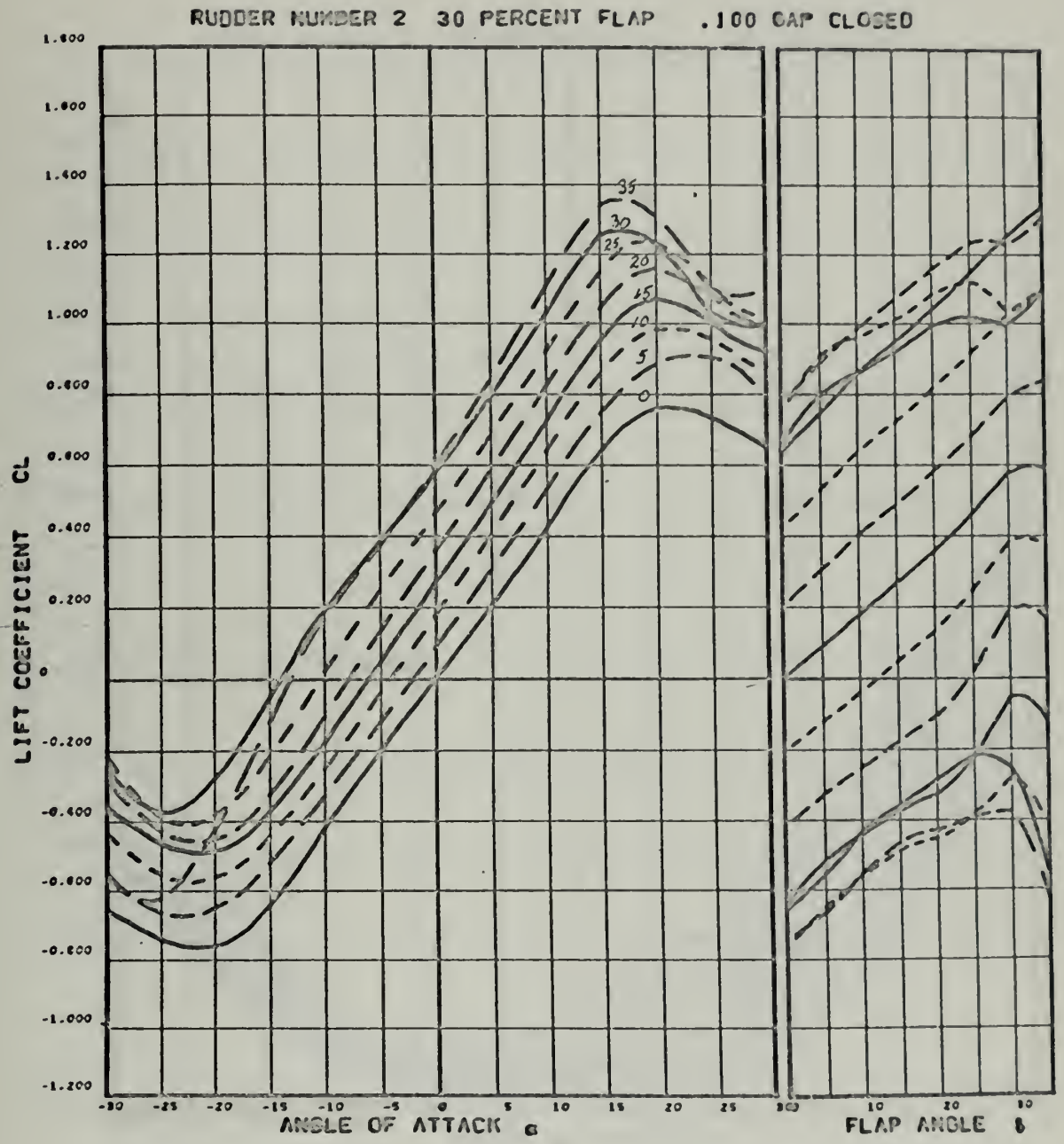
RUDDER NUMBER 2 30 PERCENT FLAP .100 GAP CLOSED
LIFT COEFFICIENT CL
1.600
1.800
1.400
1.200
1.000
0.800
0.600
0.400
0.200
0
-0.200
-0.400
-0.600
-0.800
-1.000
-1.200
35
30
25
20
15
10
5
0
-30 -25 -20 -15 -10 -5 0 5 10 15 20 25 30
ANGLE OF ATTACK α
10 20 30
FLAP ANGLE δ

Figure 8

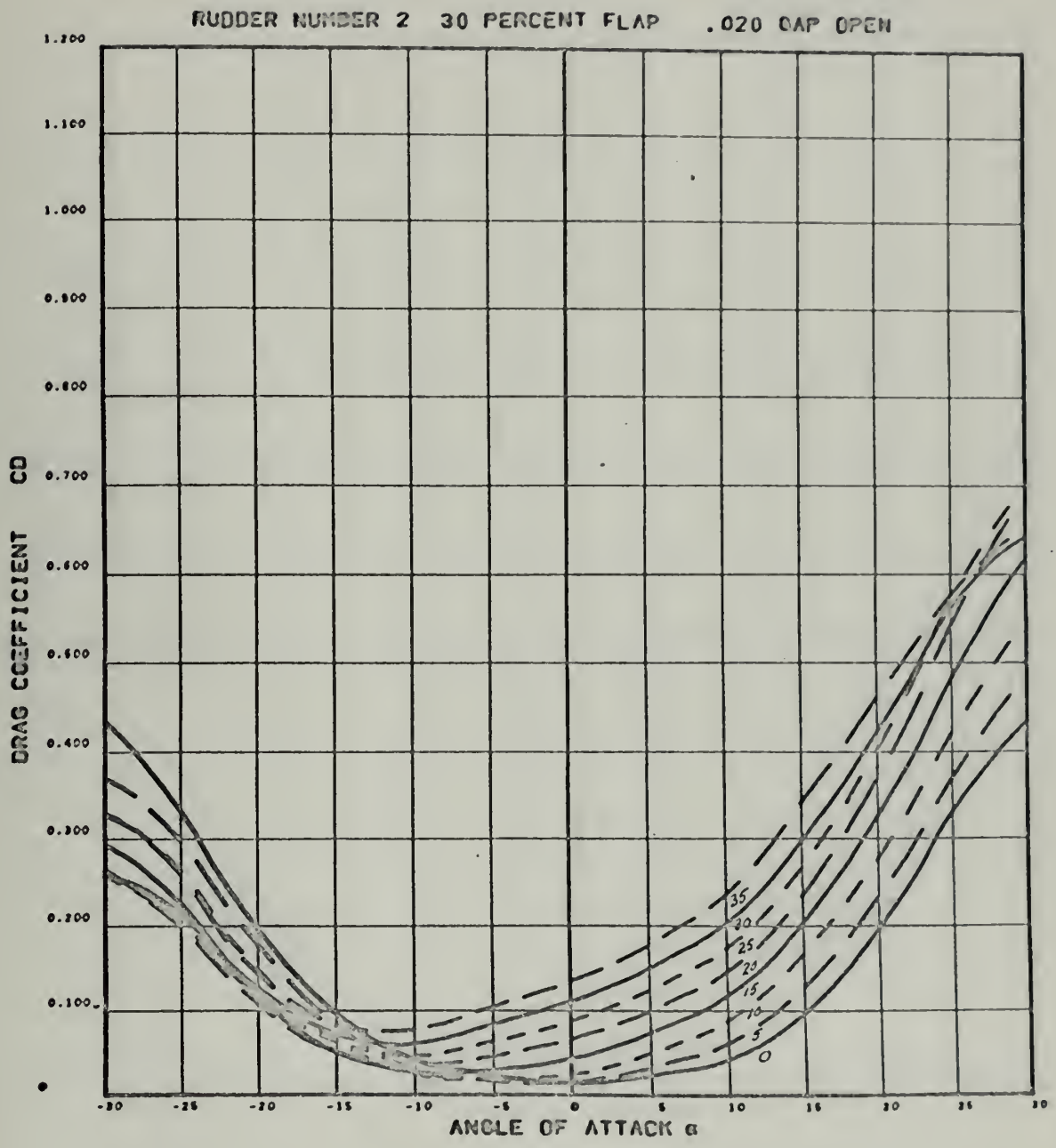
RUDDER NUMBER 2 30 PERCENT FLAP .020 GAP OPEN
DRAG COEFFICIENT CD
1.200
1.100
1.000
0.900
0.800
0.700
0.600
0.500
0.400
0.300
0.200
0.100
35
30
25
20
15
10
5
0
-30 -25 -20 -15 -10 -5 0 5 10 15 20 25 30
ANGLE OF ATTACK α

Figure 9

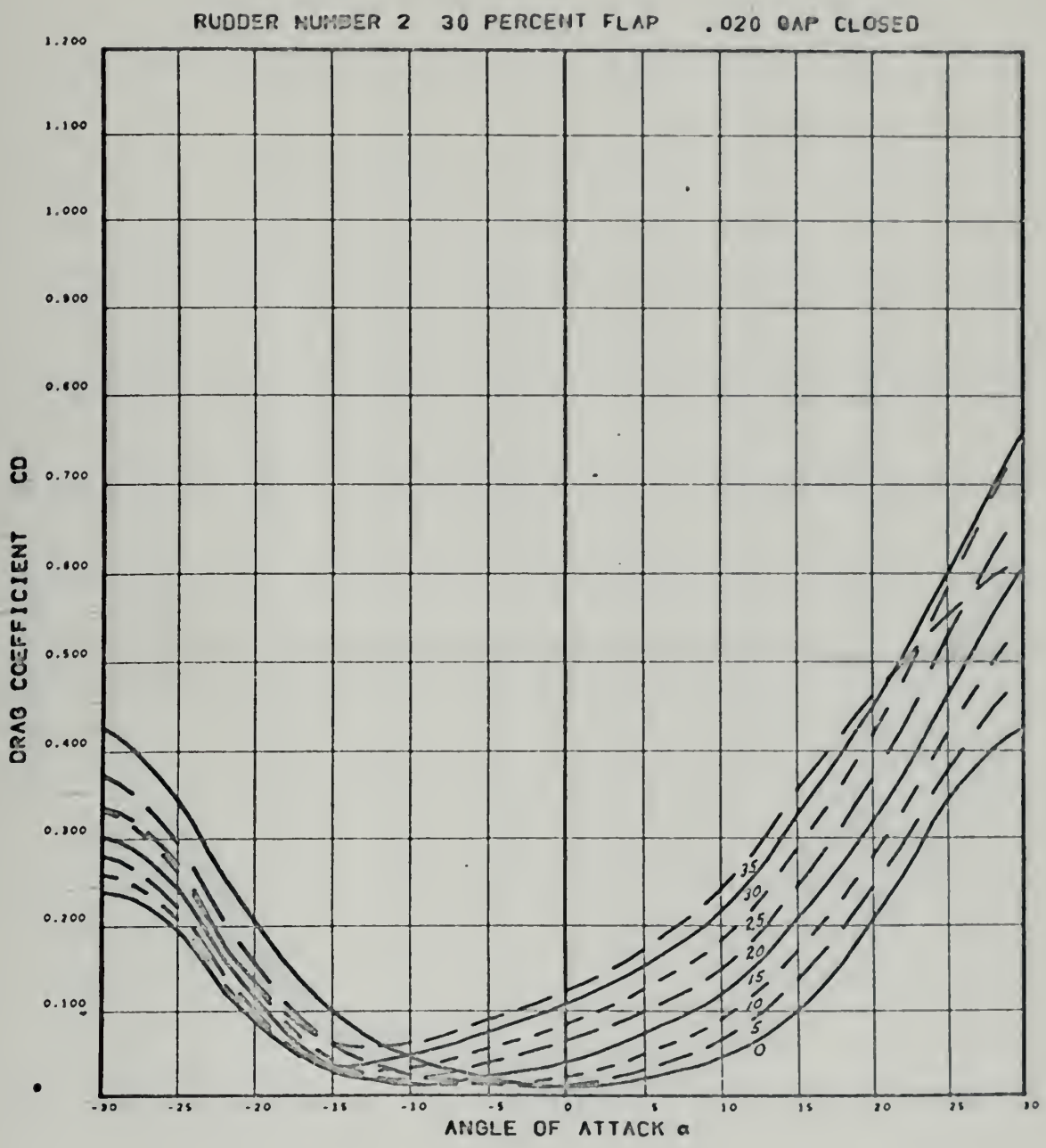
RUDDER NUMBER 2 30 PERCENT FLAP .020 GAP CLOSED
DRAG COEFFICIENT CD
1.200
1.100
1.000
0.900
0.800
0.700
0.600
0.500
0.400
0.300
0.200
0.100
-30 -25 -20 -15 -10 -5 0 5 10 15 20 25 30
ANGLE OF ATTACK α
35
30
25
20
15
10
5
0

Figure 10

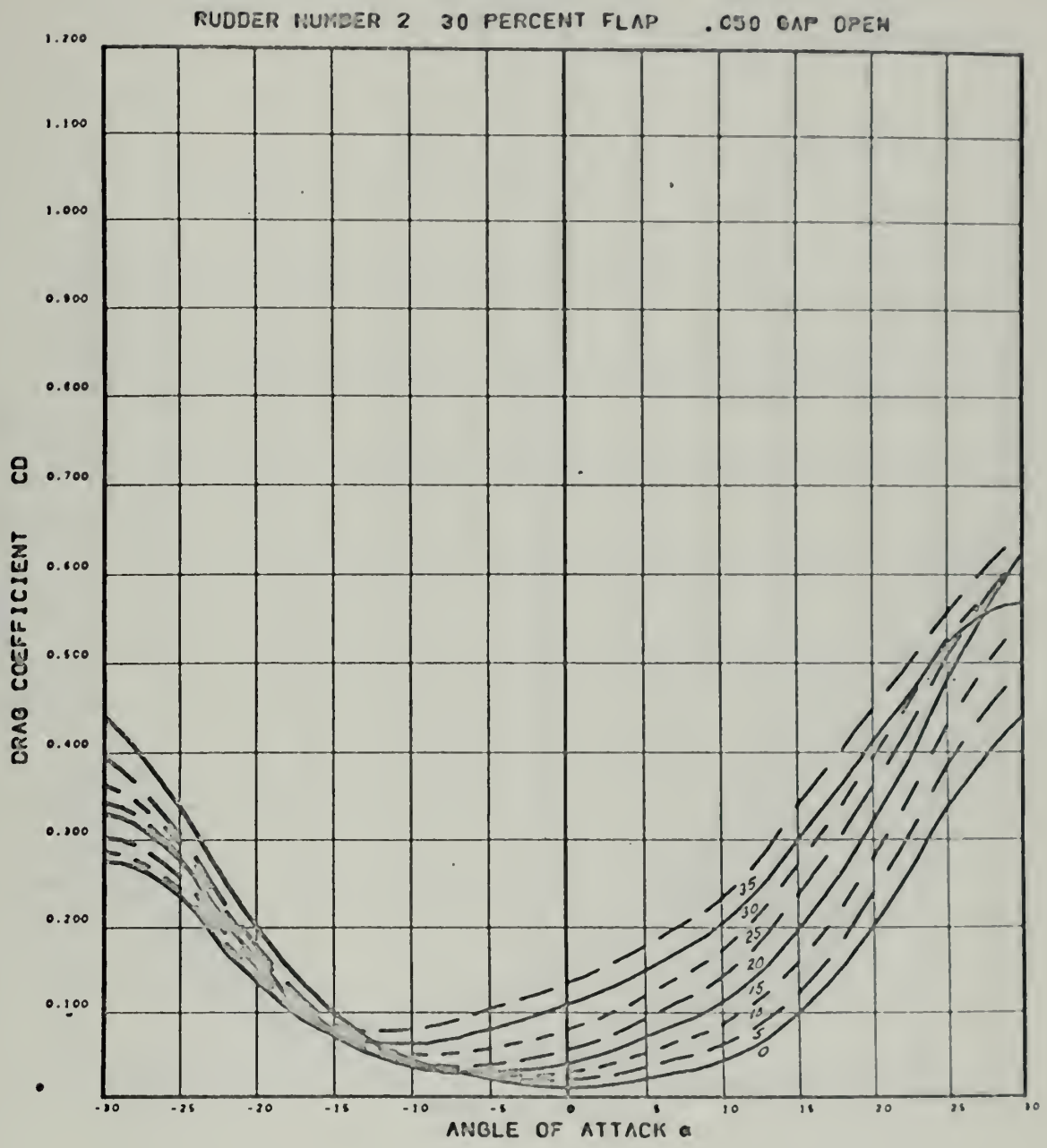
RUDDER NUMBER 2 30 PERCENT FLAP .050 GAP OPEN
DRAG COEFFICIENT CD
1.200
1.100
1.000
0.900
0.800
0.700
0.600
0.500
0.400
0.300
0.200
0.100
-30
-25
-20
-15
-10
-5
0
5
10
15
20
25
30
ANGLE OF ATTACK α
35
30
25
20
15
10
5
0

Figure 11

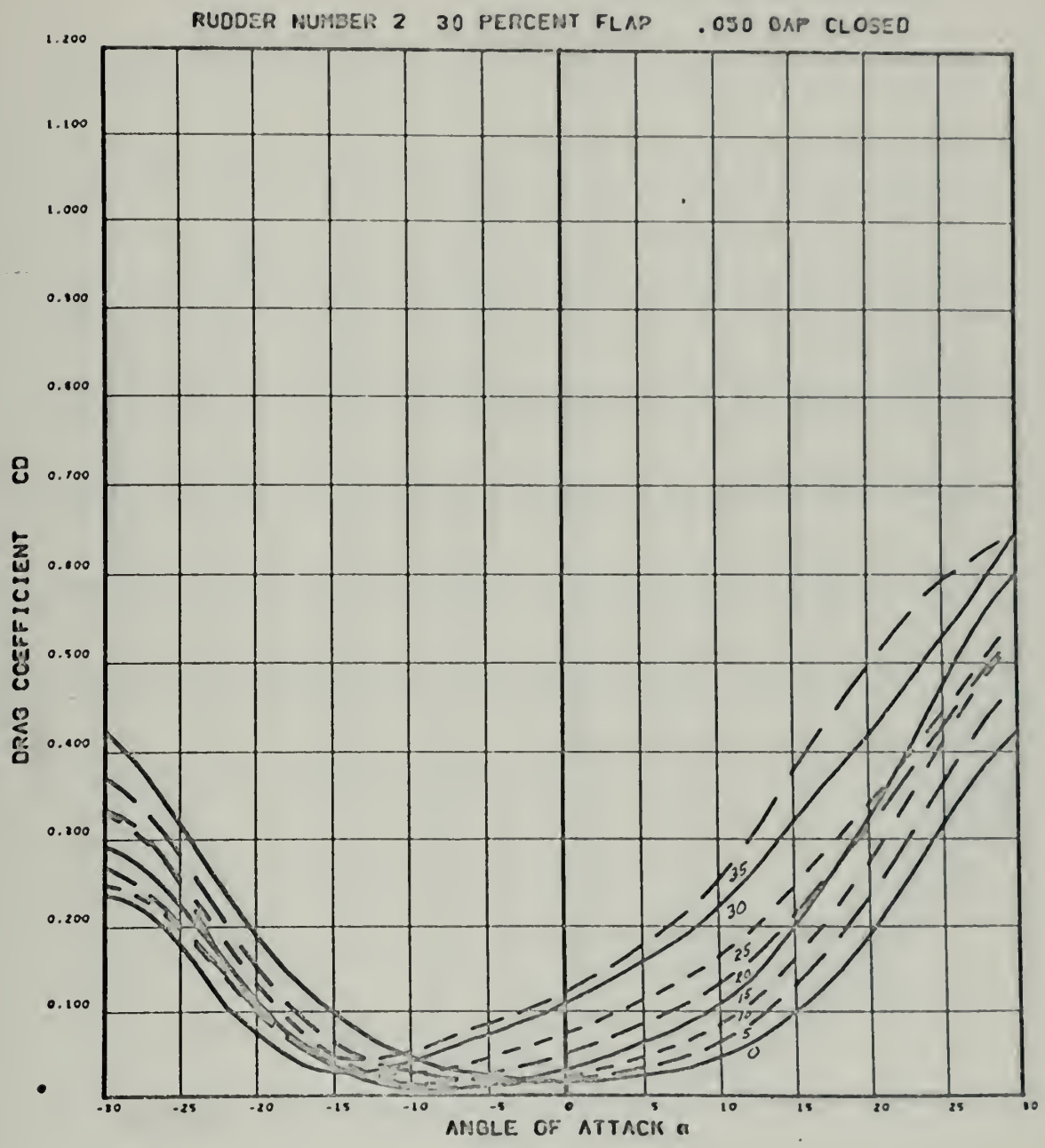
RUDDER NUMBER 2 30 PERCENT FLAP .030 GAP CLOSED
DRAG COEFFICIENT CD
1.200
1.100
1.000
0.900
0.800
0.700
0.600
0.500
0.400
0.300
0.200
0.100
-30
-25
-20
-15
-10
-5
0
5
10
15
20
25
30
ANGLE OF ATTACK α
35
30
25
20
15
10
5
0

Figure 12

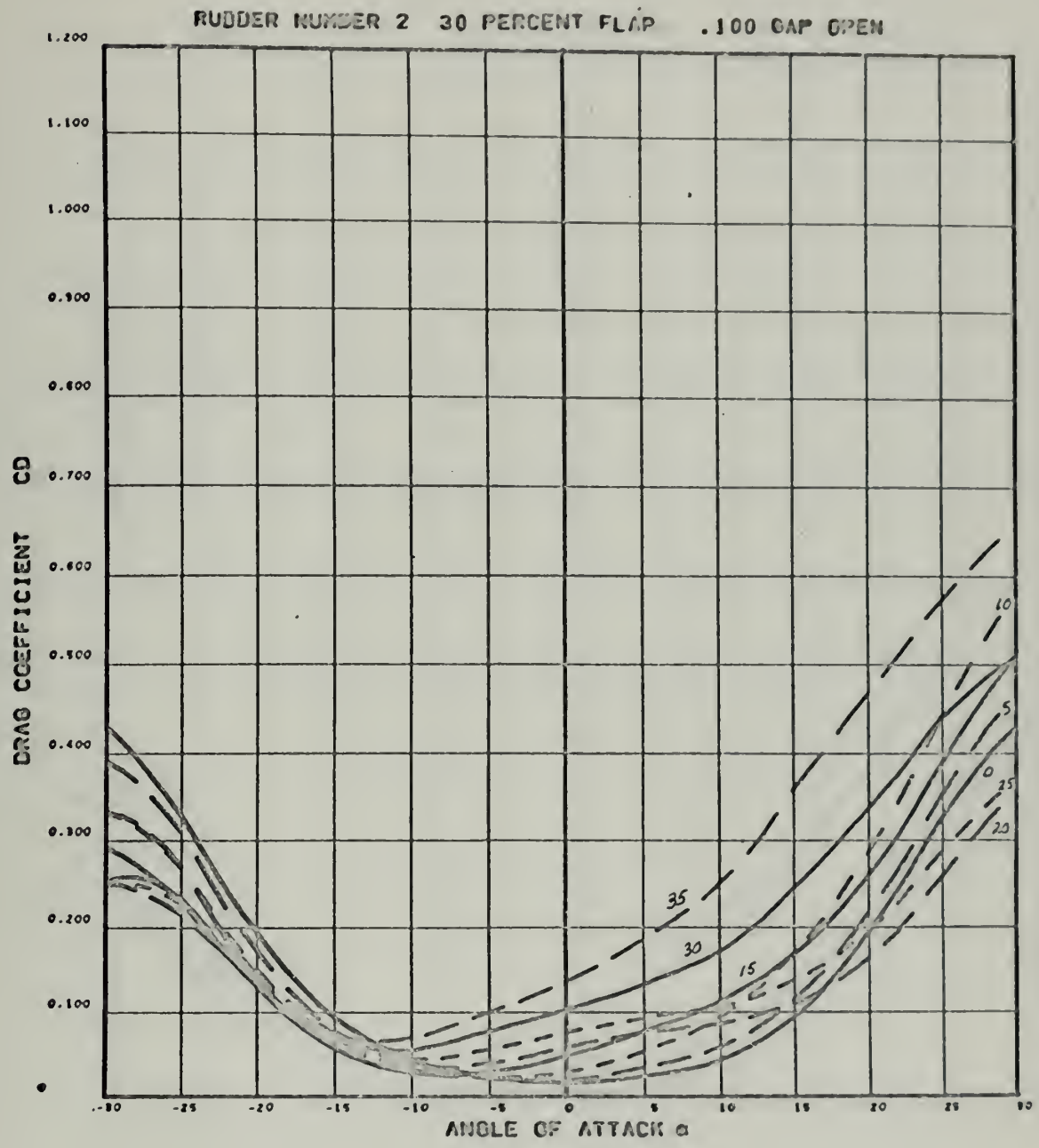
RUDDER NUMBER 2 30 PERCENT FLAP .100 GAP OPEN
DRAG COEFFICIENT CD
1.200
1.100
1.000
0.900
0.800
0.700
0.600
0.500
0.400
0.300
0.200
0.100
-30
-25
-20
-15
-10
-5
0
5
10
15
20
25
30
ANGLE OF ATTACK α
35
30
15
10
5
0
25
20

Figure 13

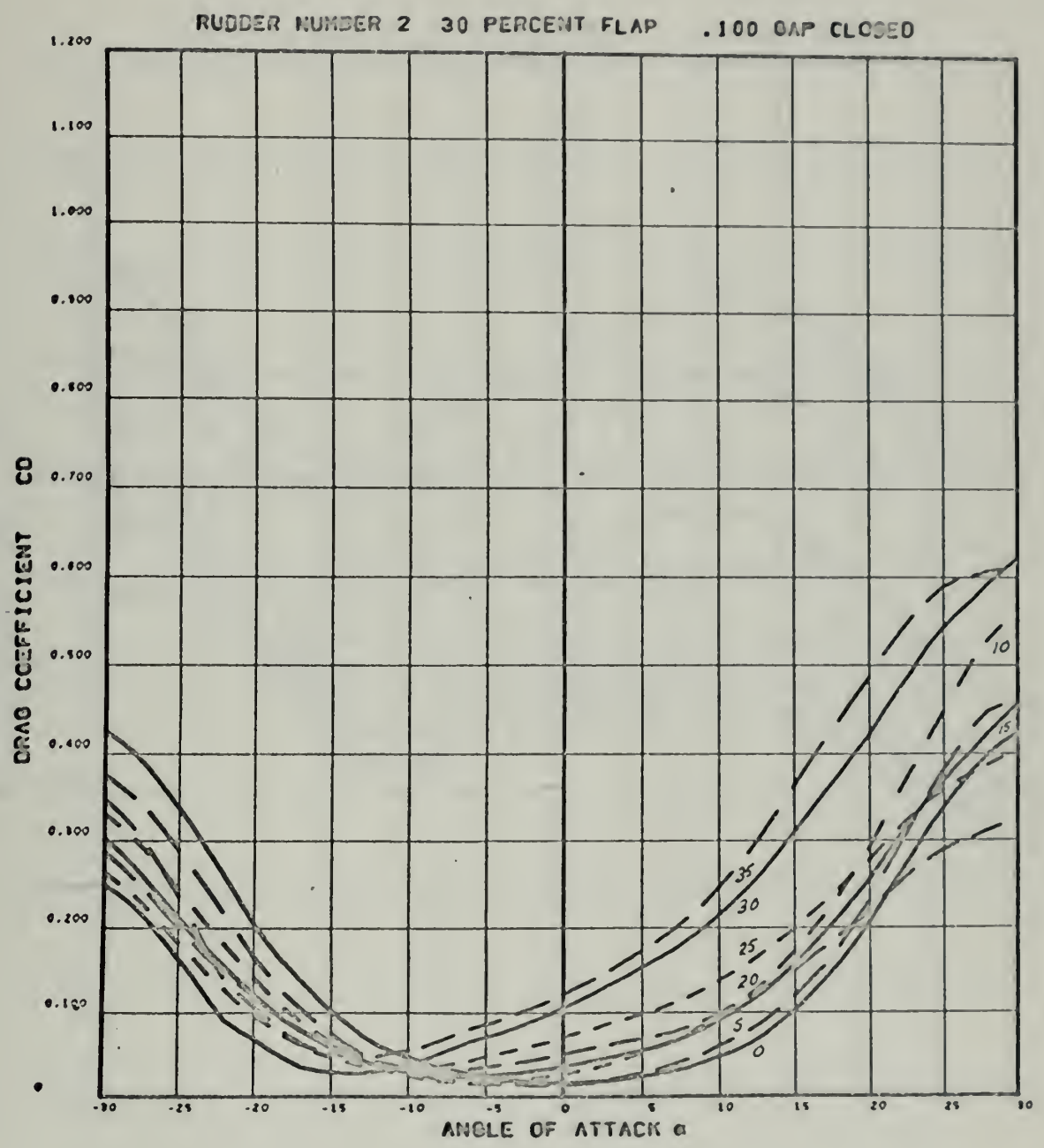
RUDDER NUMBER 2 30 PERCENT FLAP .100 GAP CLOSED
DRAG COEFFICIENT CD
1.200
1.100
1.000
0.900
0.800
0.700
0.600
0.500
0.400
0.300
0.200
0.100
-30 -25 -20 -15 -10 -5 0 5 10 15 20 25 30
ANGLE OF ATTACK α
35
30
25
20
15
10
5
0

Figure 14

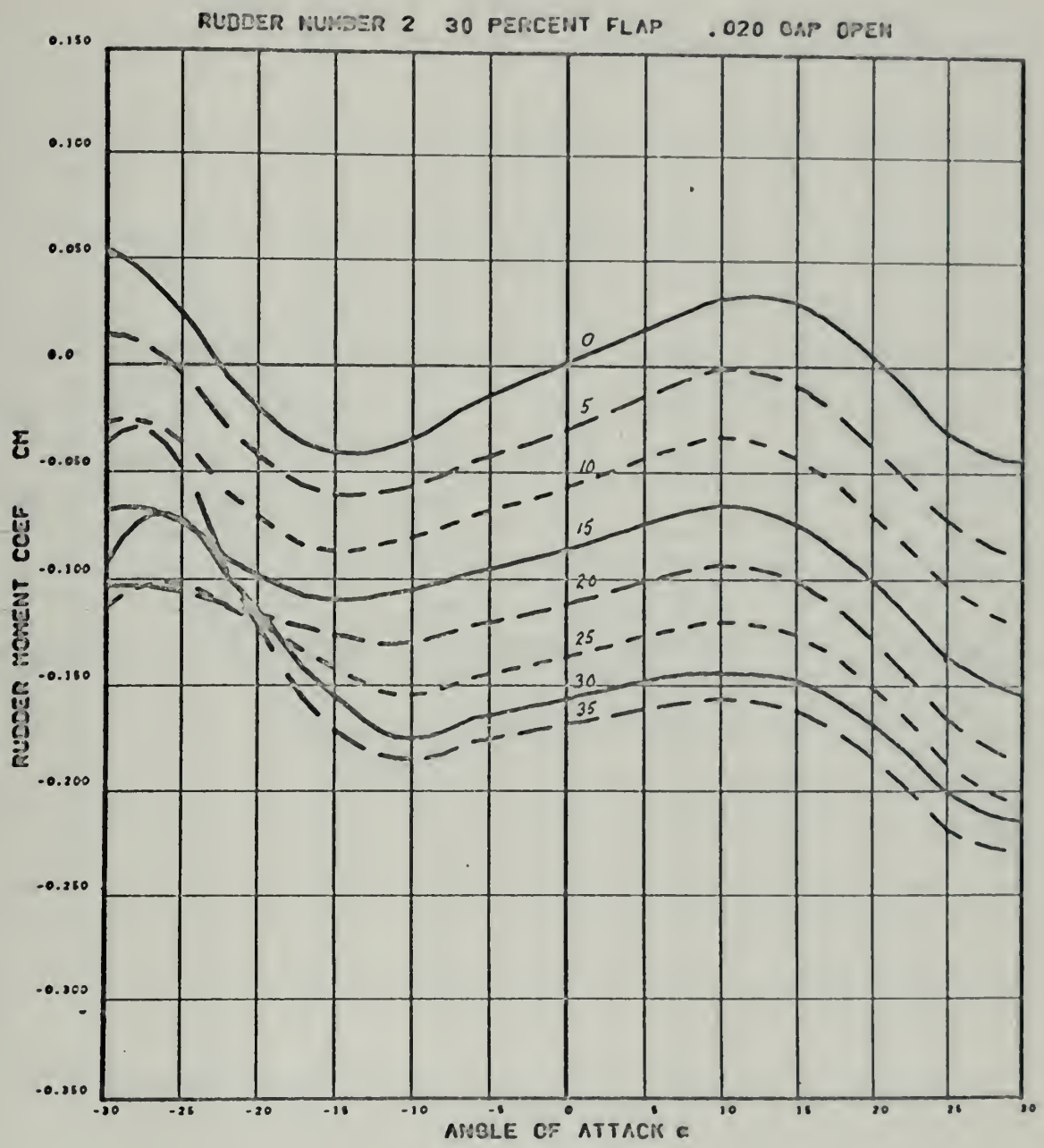
RUDDER NUMBER 2 30 PERCENT FLAP .020 GAP OPEN
RUDDER MOMENT COEF CM
0.150
0.100
0.050
0.0
-0.050
-0.100
-0.150
-0.200
-0.250
-0.300
-0.350
-30
-25
-20
-15
-10
-5
0
5
10
15
20
25
30
ANGLE OF ATTACK α
0
5
10
15
20
25
30
35

Figure 15

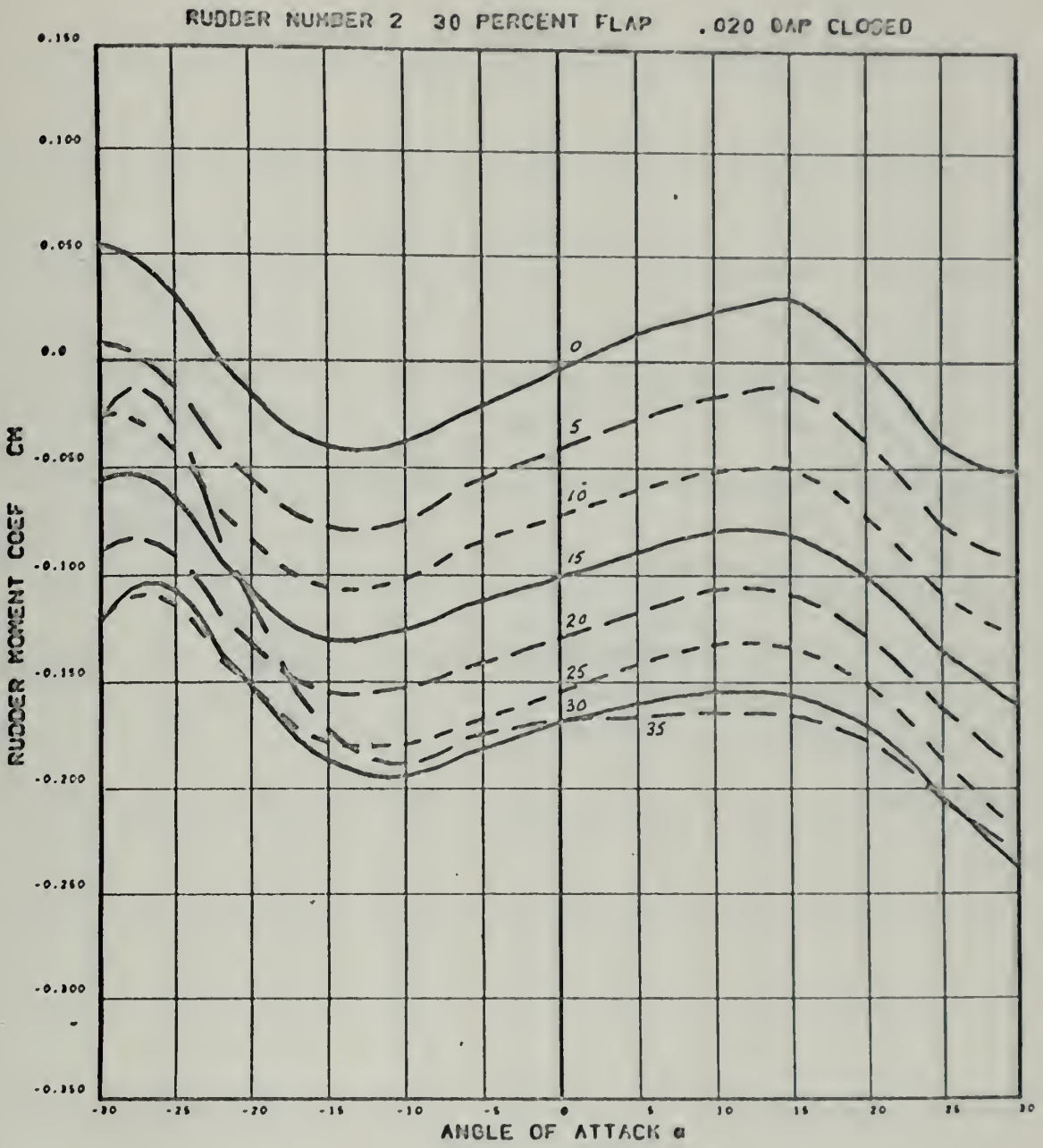
RUDDER NUMBER 2 30 PERCENT FLAP .020 GAP CLOSED
RUDDER MOMENT COEF CM
0.150
0.100
0.050
0.0
-0.050
-0.100
-0.150
-0.200
-0.250
-0.300
-0.350
-30
-25
-20
-15
-10
-5
0
5
10
15
20
25
30
ANGLE OF ATTACK α
0
5
10
15
20
25
30
35

Figure 16

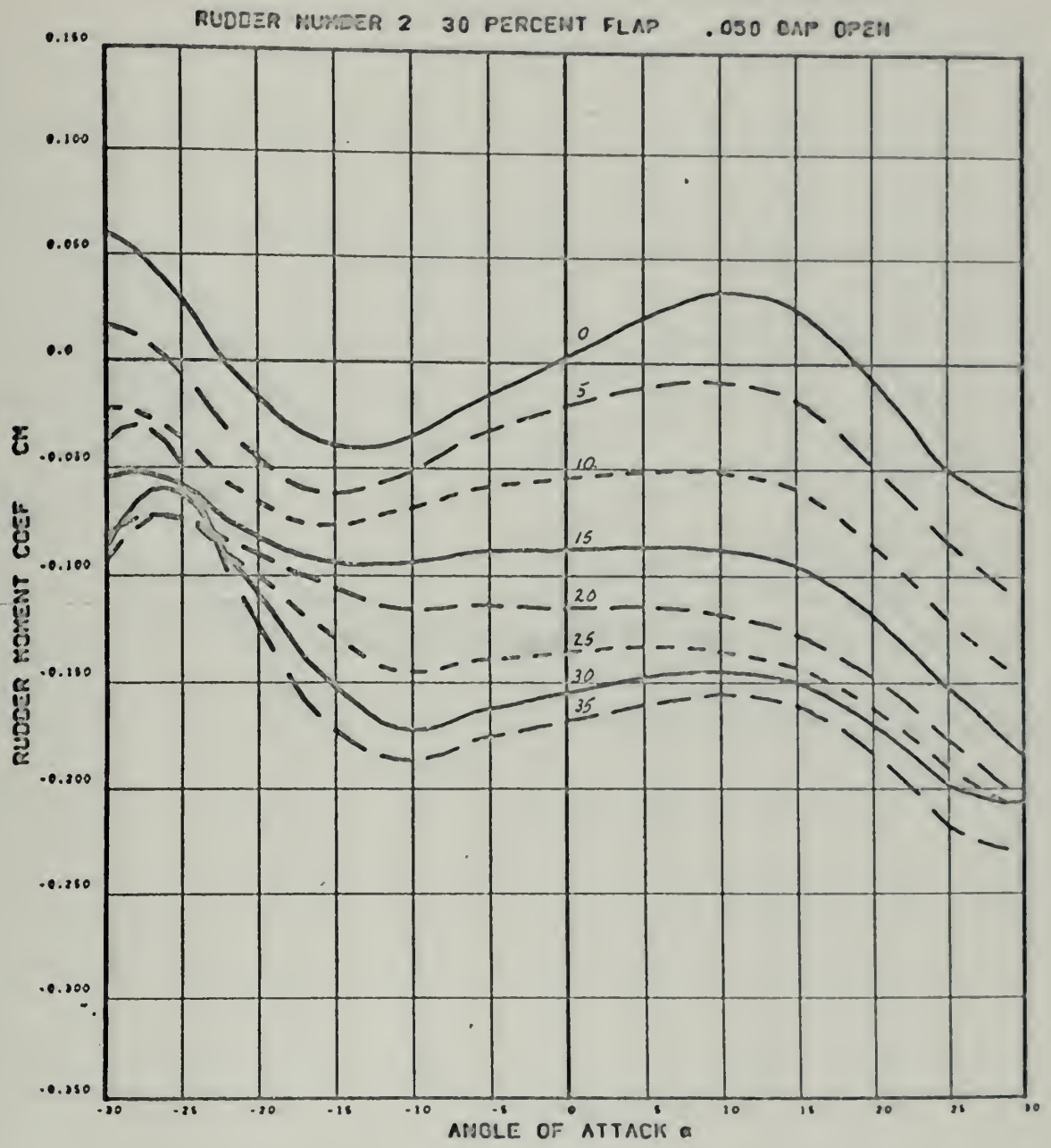
RUDDER NUMBER 2 30 PERCENT FLAP .050 GAP OPEN
RUDDER MOMENT COEF CM
0.150
0.100
0.050
0.0
-0.050
-0.100
-0.150
-0.200
-0.250
-0.300
-0.350
0
5
10
15
20
25
30
35
-30
-25
-20
-15
-10
-5
0
5
10
15
20
25
30
ANGLE OF ATTACK α

Figure 17

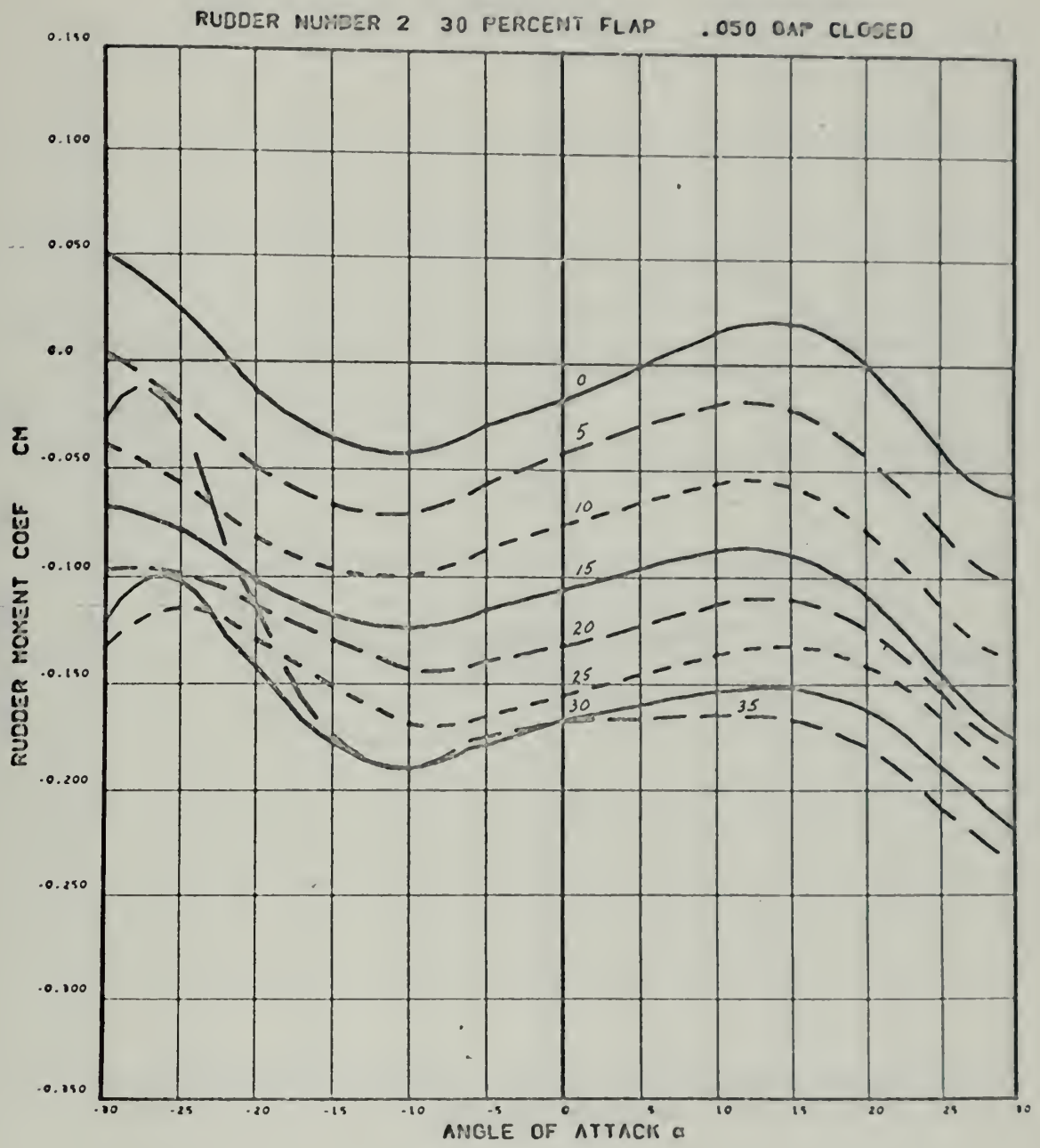
RUDDER NUMBER 2 30 PERCENT FLAP .050 GAP CLOSED
RUDDER MOMENT COEF CM
0.150
0.100
0.050
0.0
-0.050
-0.100
-0.150
-0.200
-0.250
-0.300
-0.350
-30
-25
-20
-15
-10
-5
0
5
10
15
20
25
30
0
5
10
15
20
25
30
35
ANGLE OF ATTACK α

Figure 18

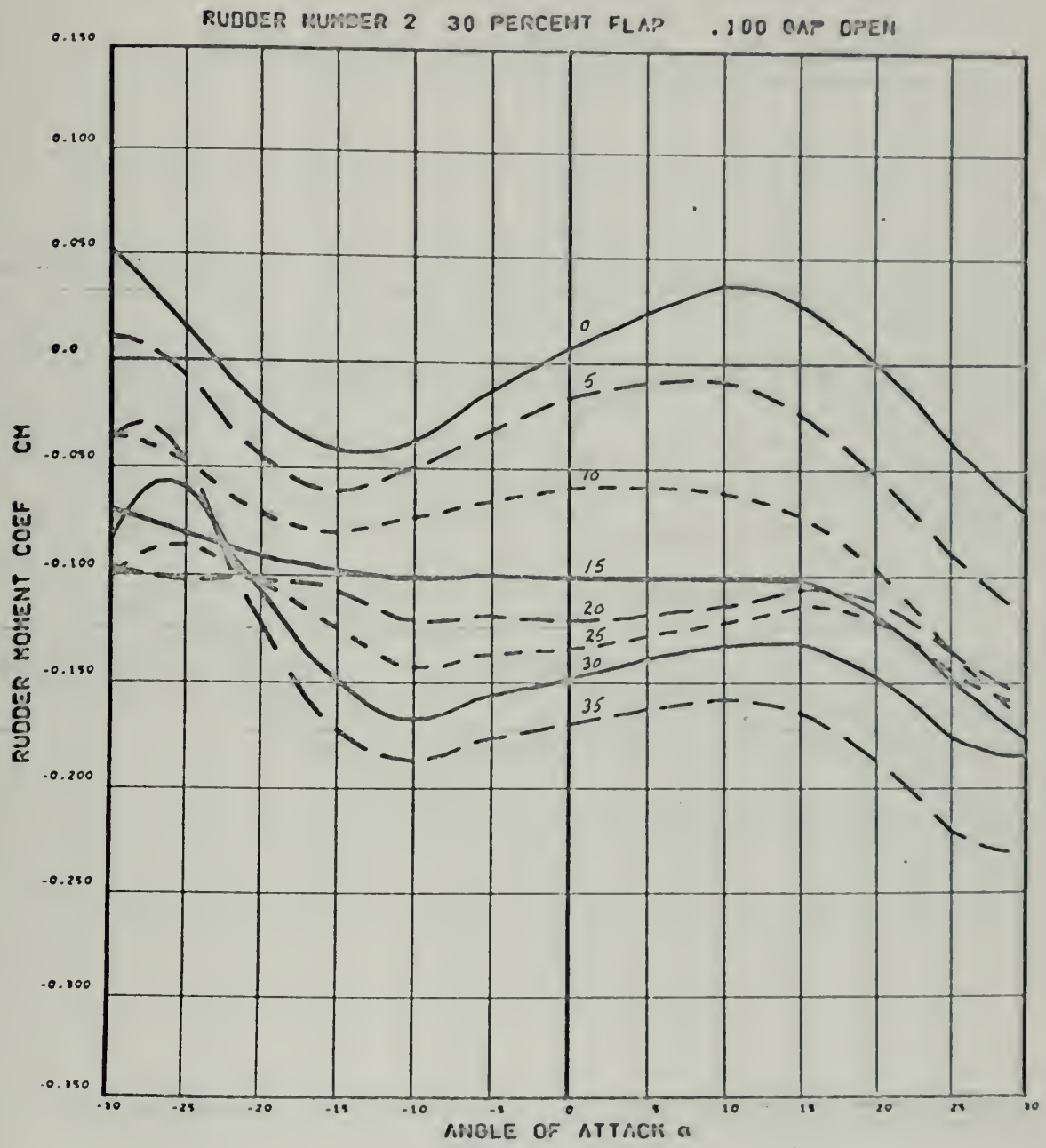
RUDDER NUMBER 2 30 PERCENT FLAP .100 GAP OPEN
RUDDER MOMENT COEF CM
0.150
0.100
0.050
0.0
-0.050
-0.100
-0.150
-0.200
-0.250
-0.300
-0.350
-30
-25
-20
-15
-10
-5
0
5
10
15
20
25
30
ANGLE OF ATTACK α
0
5
10
15
20
25
30
35

Figure 19

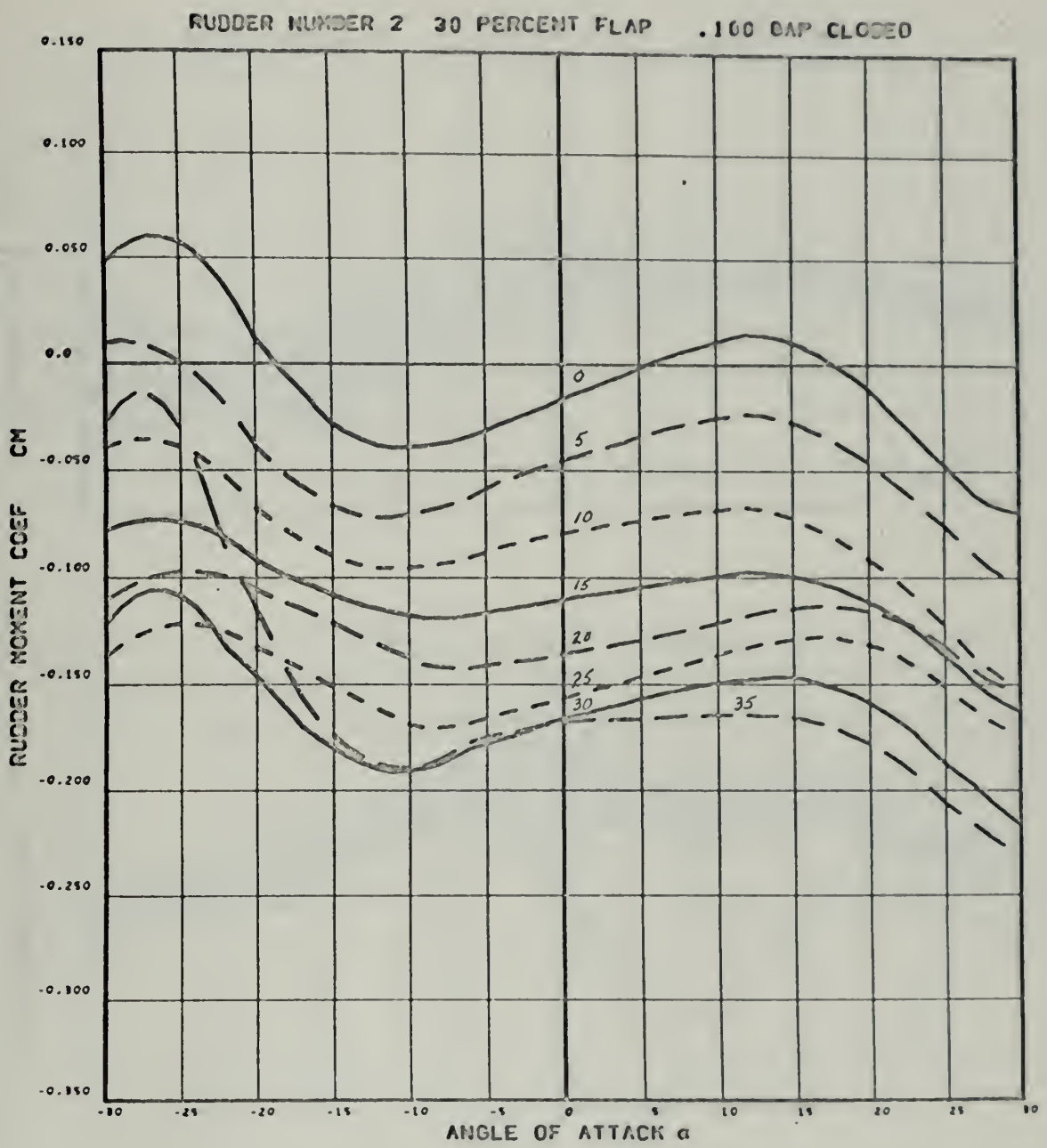
RUDDER NUMBER 2 30 PERCENT FLAP .100 GAP CLOSED
0.150
0.100
0.050
0.0
-0.050
-0.100
-0.150
-0.200
-0.250
-0.300
-0.350
RUDDER MOMENT COEF CM
0
5
10
15
20
25
30
35
-30
-25
-20
-15
-10
-5
0
5
10
15
20
25
30
ANGLE OF ATTACK α

Figure 20

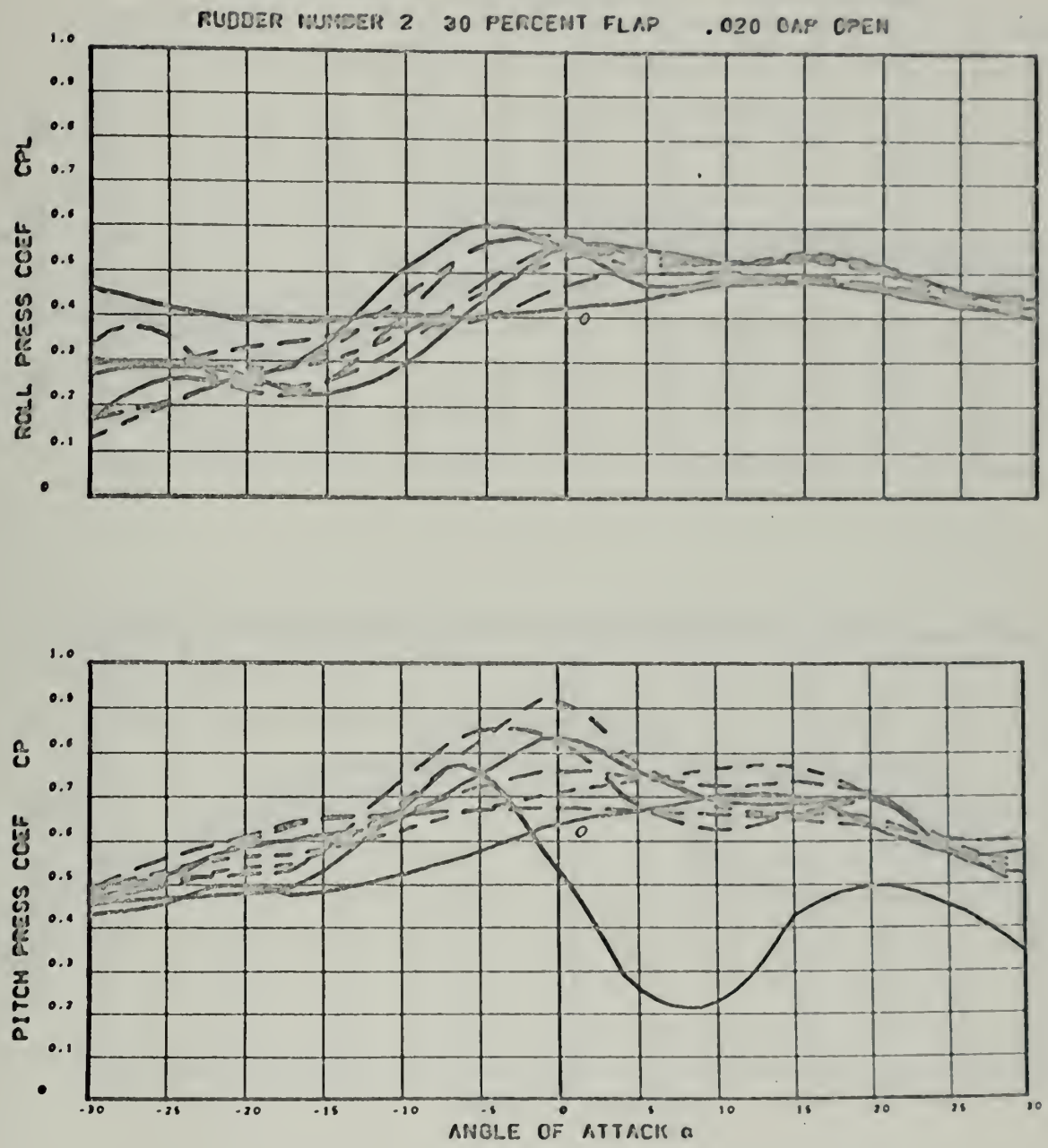
RUDDER NUMBER 2 30 PERCENT FLAP .020 GAP OPEN
ROLL PRESS COEF CPL
1.0
0.9
0.8
0.7
0.6
0.5
0.4
0.3
0.2
0.1
0
PITCH PRESS COEF CP
-30
-25
-20
-15
-10
-5
0
5
10
15
20
25
30
ANGLE OF ATTACK α

Figure 21

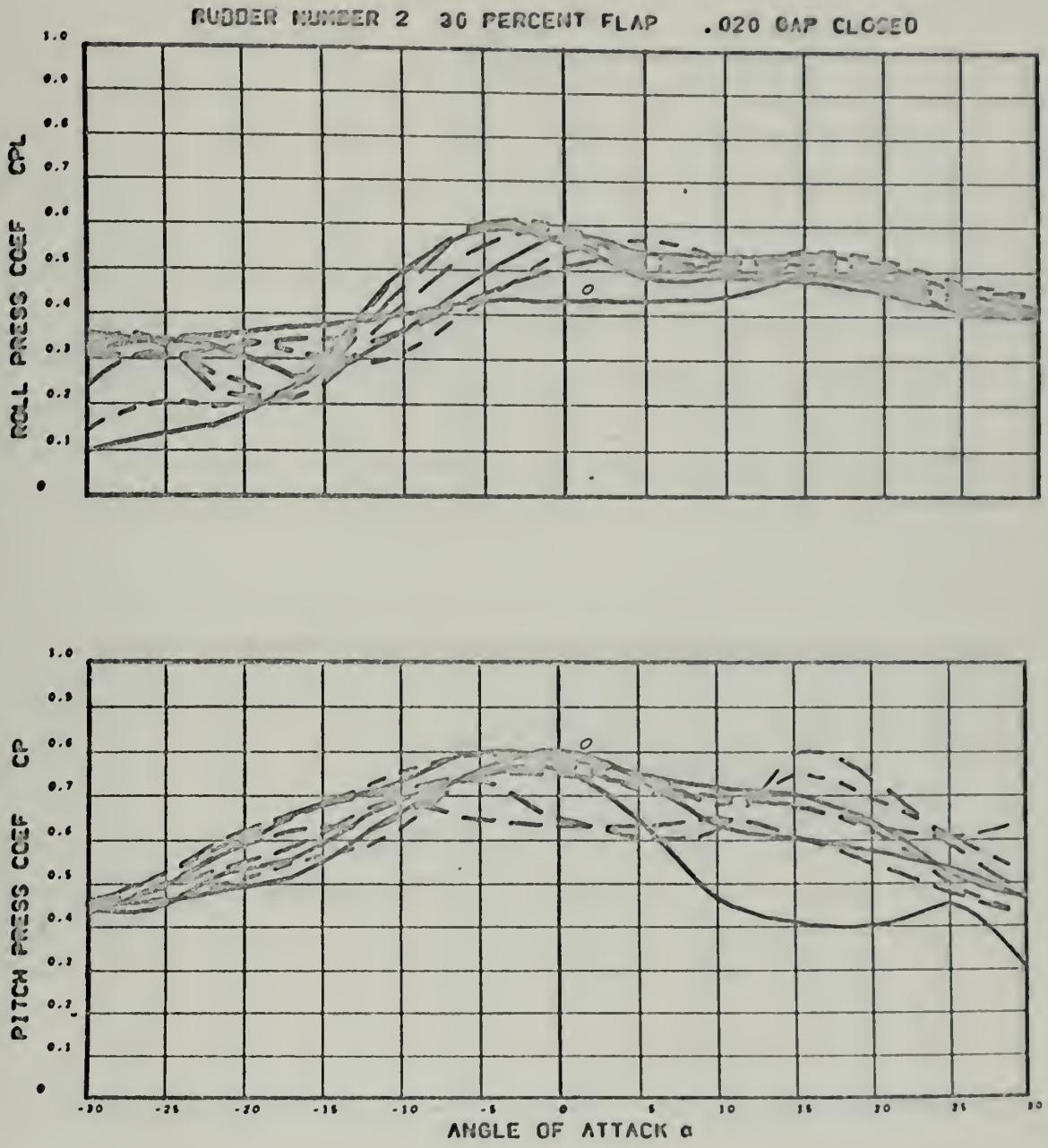
RUDDER NUMBER 2 30 PERCENT FLAP .020 GAP CLOSED
ROLL PRESS COEF CPL
PITCH PRESS COEF CP
ANGLE OF ATTACK α

Figure 22

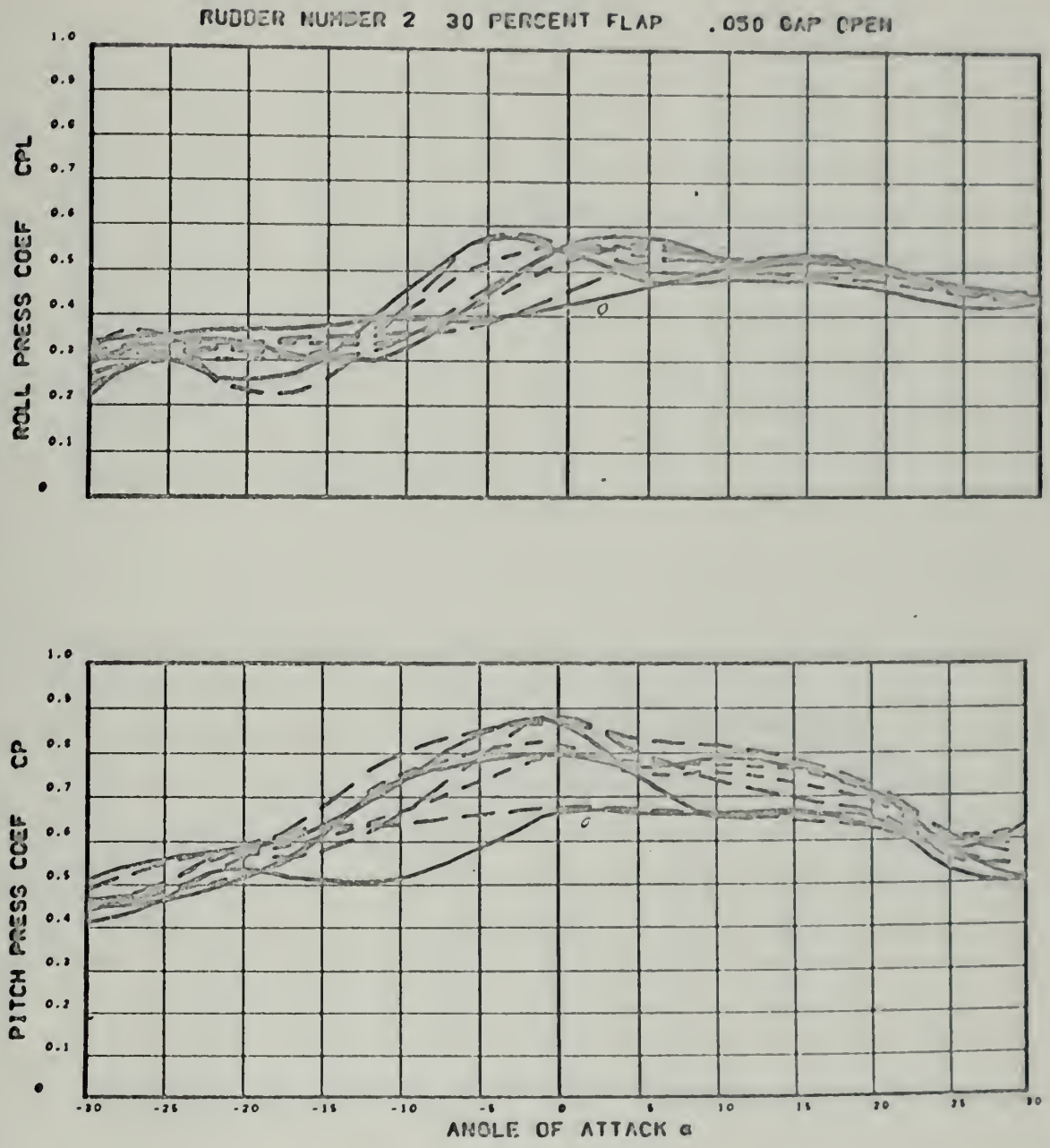
RUDDER NUMBER 2 30 PERCENT FLAP .030 GAP OPEN
ROLL PRESS COEF CPL
1.0
0.9
0.8
0.7
0.6
0.5
0.4
0.3
0.2
0.1
0
PITCH PRESS COEF CP
1.0
0.9
0.8
0.7
0.6
0.5
0.4
0.3
0.2
0.1
0
-30
-25
-20
-15
-10
-5
0
5
10
15
20
25
30
ANGLE OF ATTACK α

Figure 23

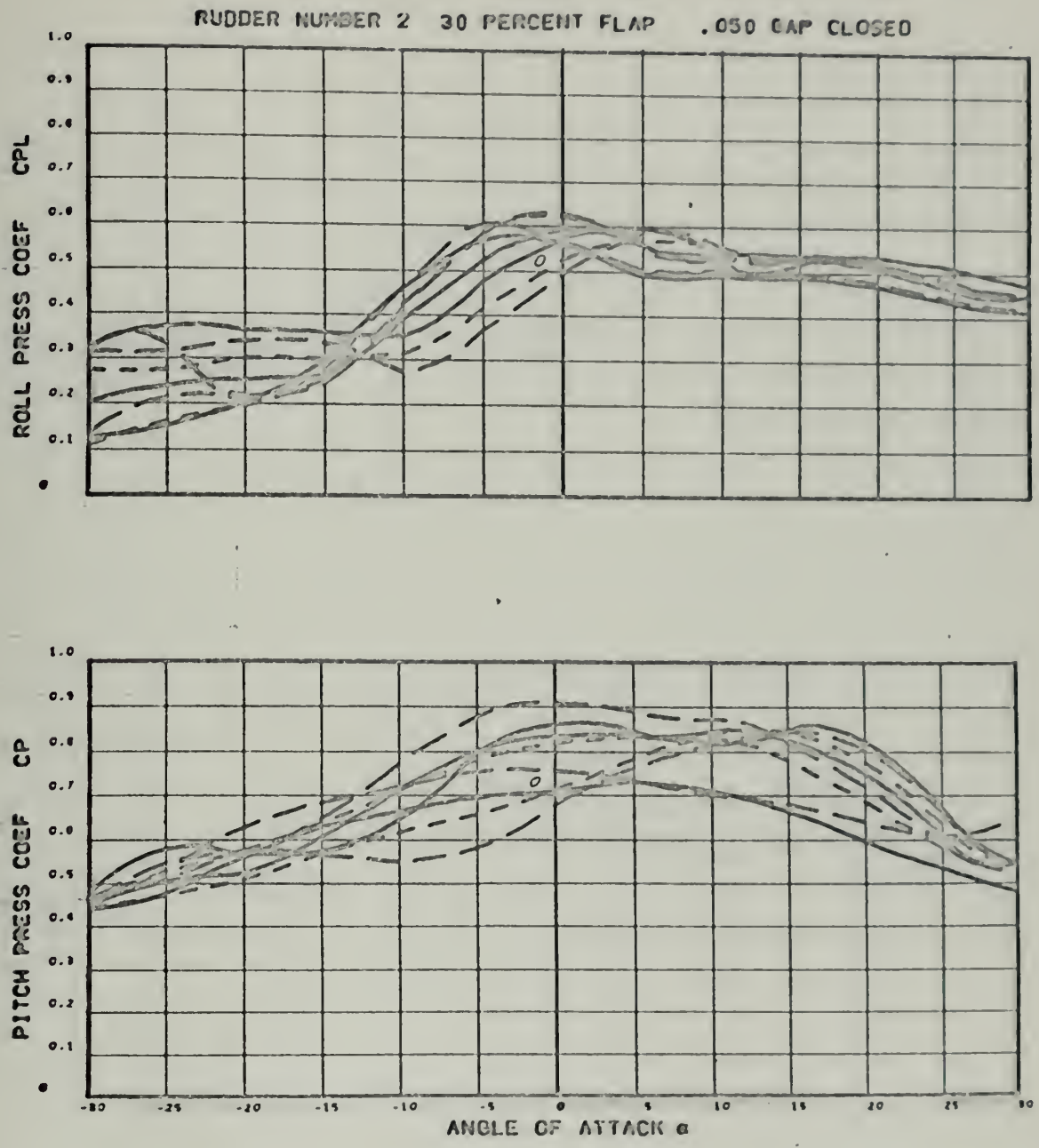
RUDDER NUMBER 2 30 PERCENT FLAP .050 GAP CLOSED
ROLL PRESS COEF CPL
1.0
0.9
0.8
0.7
0.6
0.5
0.4
0.3
0.2
0.1
0
PITCH PRESS COEF CP
1.0
0.9
0.8
0.7
0.6
0.5
0.4
0.3
0.2
0.1
0
-30 -25 -20 -15 -10 -5 0 5 10 15 20 25 30
ANGLE OF ATTACK α

Figure 24

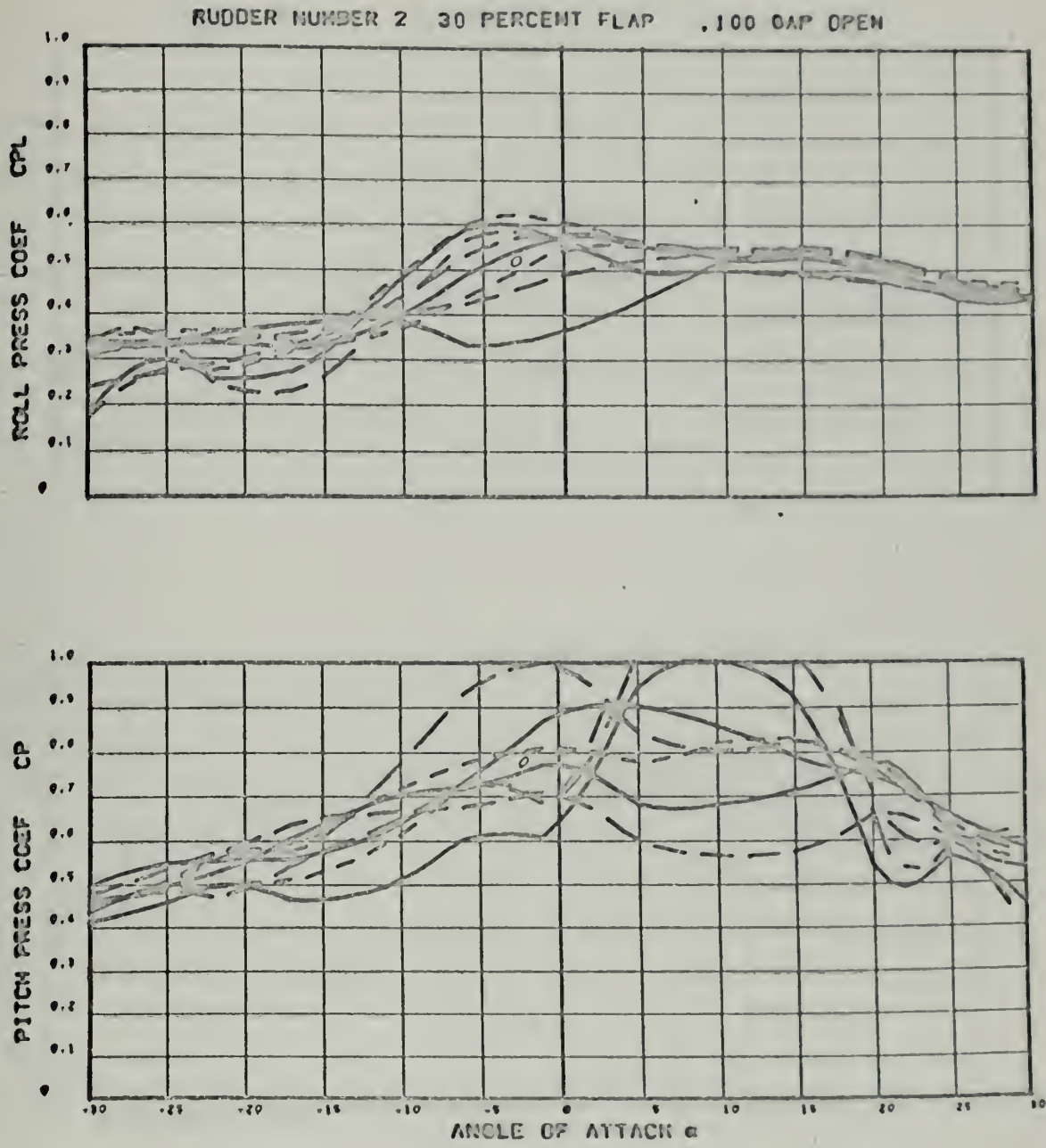
RUDDER NUMBER 2 30 PERCENT FLAP .100 GAP OPEN
ROLL PRESS COEF CPL
PITCH PRESS COEF CP
ANGLE OF ATTACK α

Figure 25

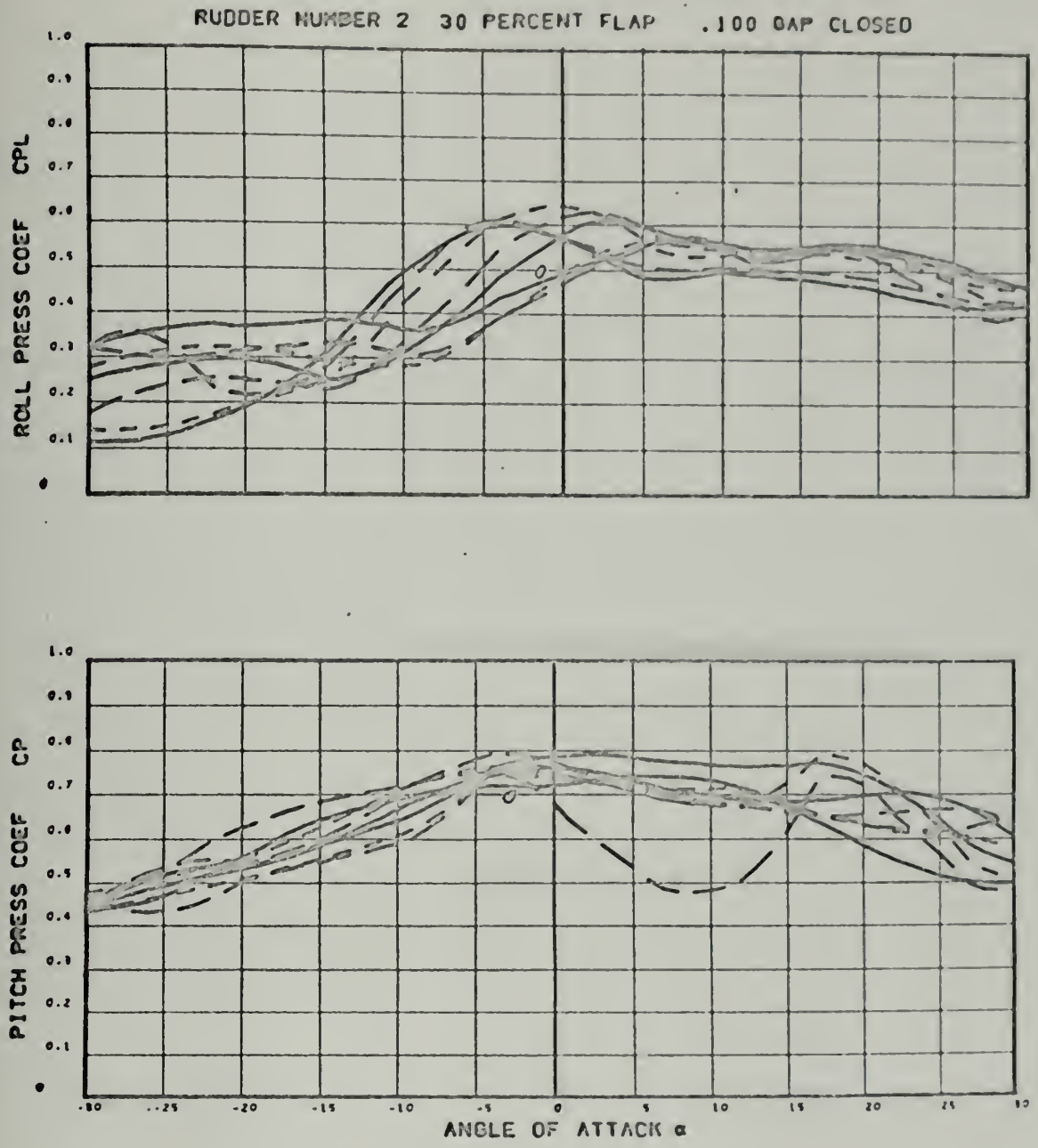
RUDDER NUMBER 2 30 PERCENT FLAP .100 GAP CLOSED
ROLL PRESS COEF CPL
1.0
0.9
0.8
0.7
0.6
0.5
0.4
0.3
0.2
0.1
0
PITCH PRESS COEF CP
1.0
0.9
0.8
0.7
0.6
0.5
0.4
0.3
0.2
0.1
0
-30
-25
-20
-15
-10
-5
0
5
10
15
20
25
30
ANGLE OF ATTACK α

Figure 26

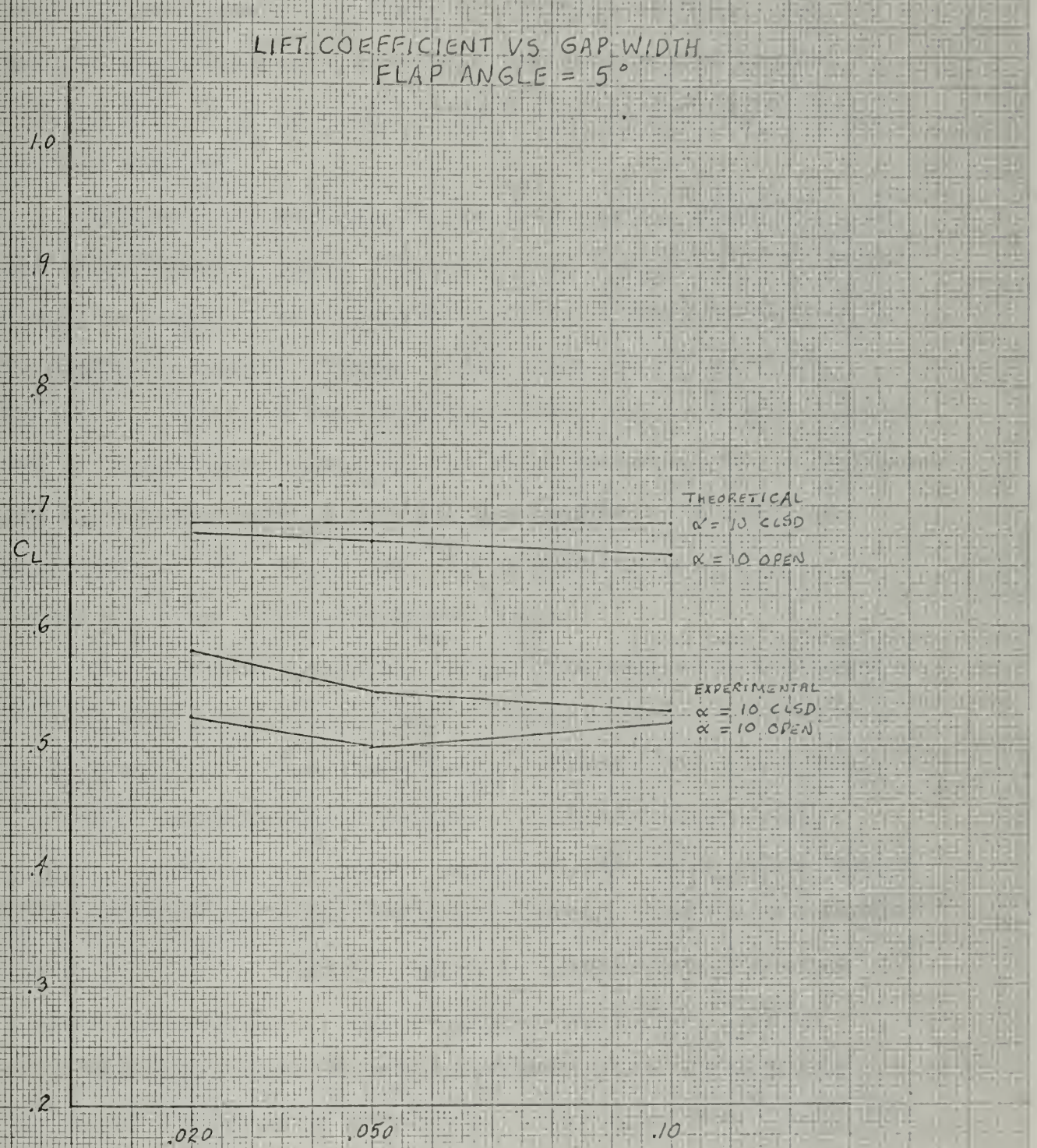
LIFT COEFFICIENT VS GAP WIDTH
FLAP ANGLE = 5°
1.0
.9
.8
.7
C_L
.6
.5
.1
.3
.2
.020
.050
.10
GAP WIDTH
THEORETICAL
α = 10 CLSD
α = 10 OPEN
EXPERIMENTAL
α = 10 CLSD
α = 10 OPEN

IV. DISCUSSION OF RESULTS

To limit this discussion to the rudder angles and flap angles normally applied to a control surface, the results are considered in detail for an angle of attack ranging from 0 to 15 degrees and a flap angle ranging from 0 to 20 degrees.

Figure 26 is a graph of the theoretical prediction and the experimental result regarding lift coefficient variation with gap width at the specification of 5 degrees flap, and 10 degrees angle of attack. This graph illustrates the following: (1) that the theoretical and experimental results are in agreement concerning the relative magnitude of closed gap C_L and open gap C_L for all gap widths. (2) that the magnitude of the theoretical C_L is greater than that resulting from the experimental tests.

The second observation is probably tha result of cross flow at the root of the model despite efforts to eliminate it by means of a root cover plate. Mechanical clearances preclude the complete elimination of cross flow by this method, although the author considers the cover plate method economically effective. The theoretical prediction assumes no cross flow at the root which in effect introduces an aspect ratio equal to twice that of the actual rudder.

For discussion of lift coefficient the results are plotted as figures 27 through 31. The following trends are evident:

(1) For a flap angle of 0 degrees the variation of C_L with gap width is slight and the differences in lift coefficient for an open or closed gap is negligible. This holds for each alpha ranging from 0 to 15 degrees.
(2) Generally for a flap angle equal to 5 degrees the open large width gap yields equivalent lift coefficients as the smaller closed gap, except at alpha of 5 degrees.
(3) For a flap angle equal to 10 degrees the larger open gap is associated with a lift coefficient greater than or equal to the smaller open or closed gap for alpha of 10 or 15 degrees. At an alpha of 5 degrees the smaller closed gap is best.
(4) For flap angles of 15 or 20 degrees the larger open gap produces larger lift coefficients than all other gap variations.

These trends of lift coefficient associated with gap variation could result from boundary-layer control at certain angular combinations of flap and rudder. Higher energy fluid is directed from the lower surface to the upper surface in such a manner as to delay separation of flow over the rudder and thus improve lift characteristics. The theoretical model assumed viscous fluid flow in the gap and ideal fluid flow in all other regions. It would seem from these results that gap effects on various characteristics would be better predicted using boundary-layer theory for

some regions of the flow field.

Figure 32 illustrates that the change of lift coefficient with the change of angle of attack is higher for larger open gaps while the flap angle varies from 5 to 20 degrees.

Considering an angle of attack range from 0 to 15 degrees, figures 8 through 13 reveal the following drag coefficient variations: (1) All differences are small; (2) Drag coefficients decrease as open gap width increases; (3) Open gap drag coefficients are less than closed gap coefficients at small gap widths. If the hydrodynamic flow is improved by extending the point of separation the drag coefficient could be expected to decrease.

There exists a tendency for an open gap rudder to have less variation in rudder moment coefficient than a closed gap rudder at the same gap width. This variation is illustrated in figures 14 through 19. Study of figures 20 through 25 reveals no noteworthy variations in lift center of pressure coefficient as the gap width is varied open or closed over an angle of attack domain from 0 to 15 degrees.

Figure 27

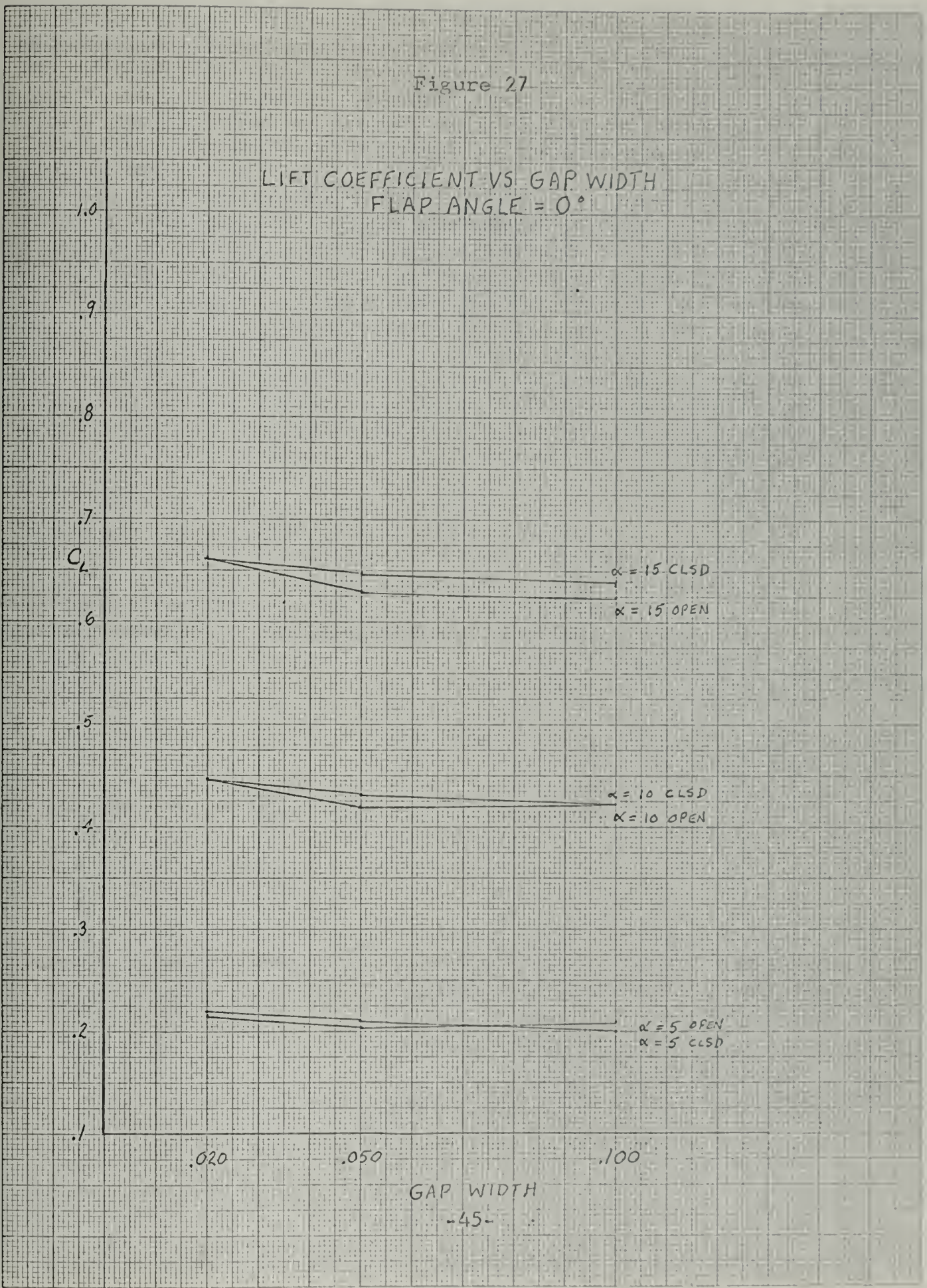
LIFT COEFFICIENT VS GAP WIDTH
FLAP ANGLE = 0°
1.0
.9
.8
.7
C_L
.6
.5
.4
.3
.2
.1
α = 15 CLSD
α = 15 OPEN
α = 10 CLSD
α = 10 OPEN
α = 5 OPEN
α = 5 CLSD
.020
.050
.100
GAP WIDTH

Figure 28

LIFT COEFFICIENT VS GAP WIDTH
FLAP ANGLE = 5°

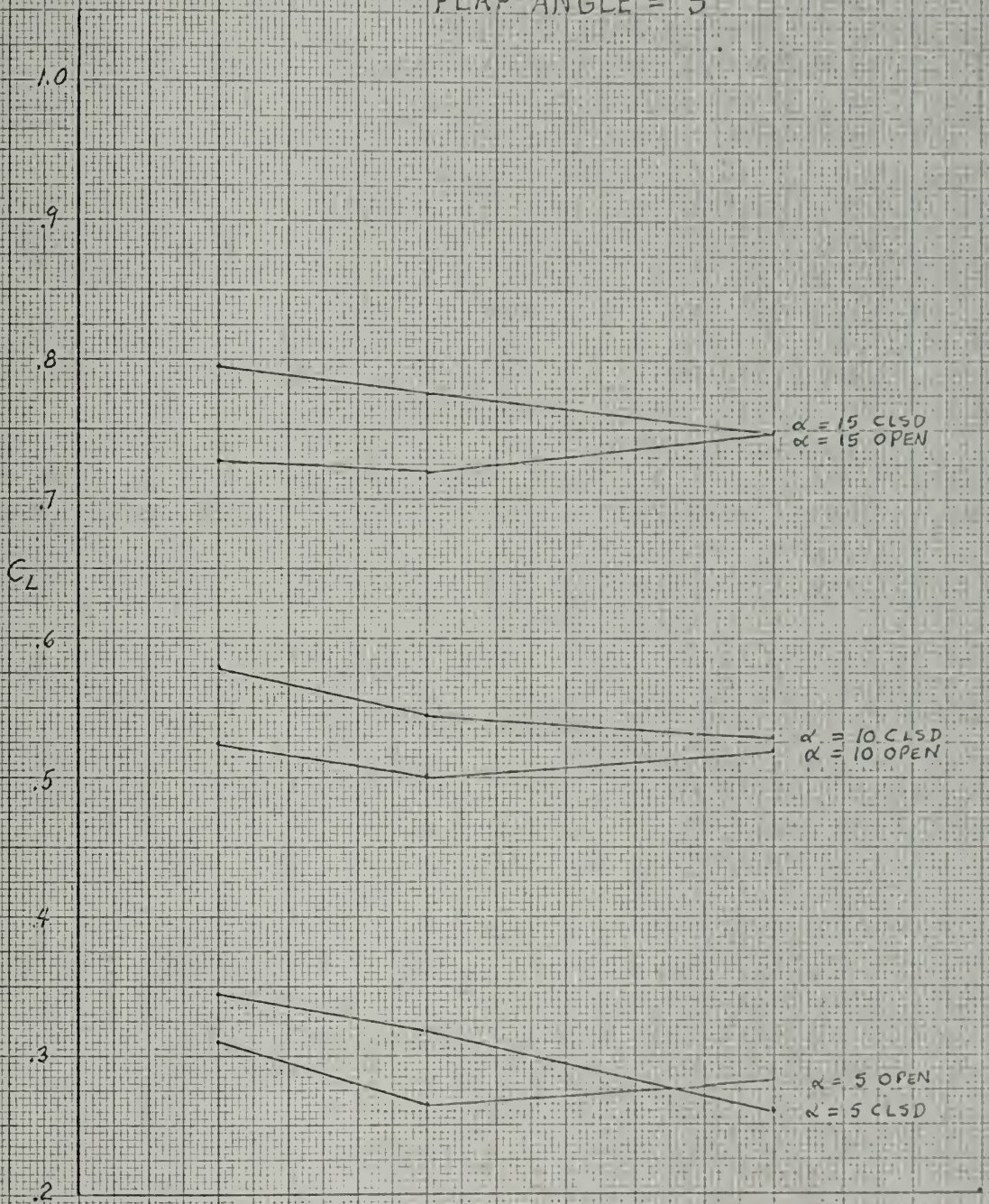

Figure 29

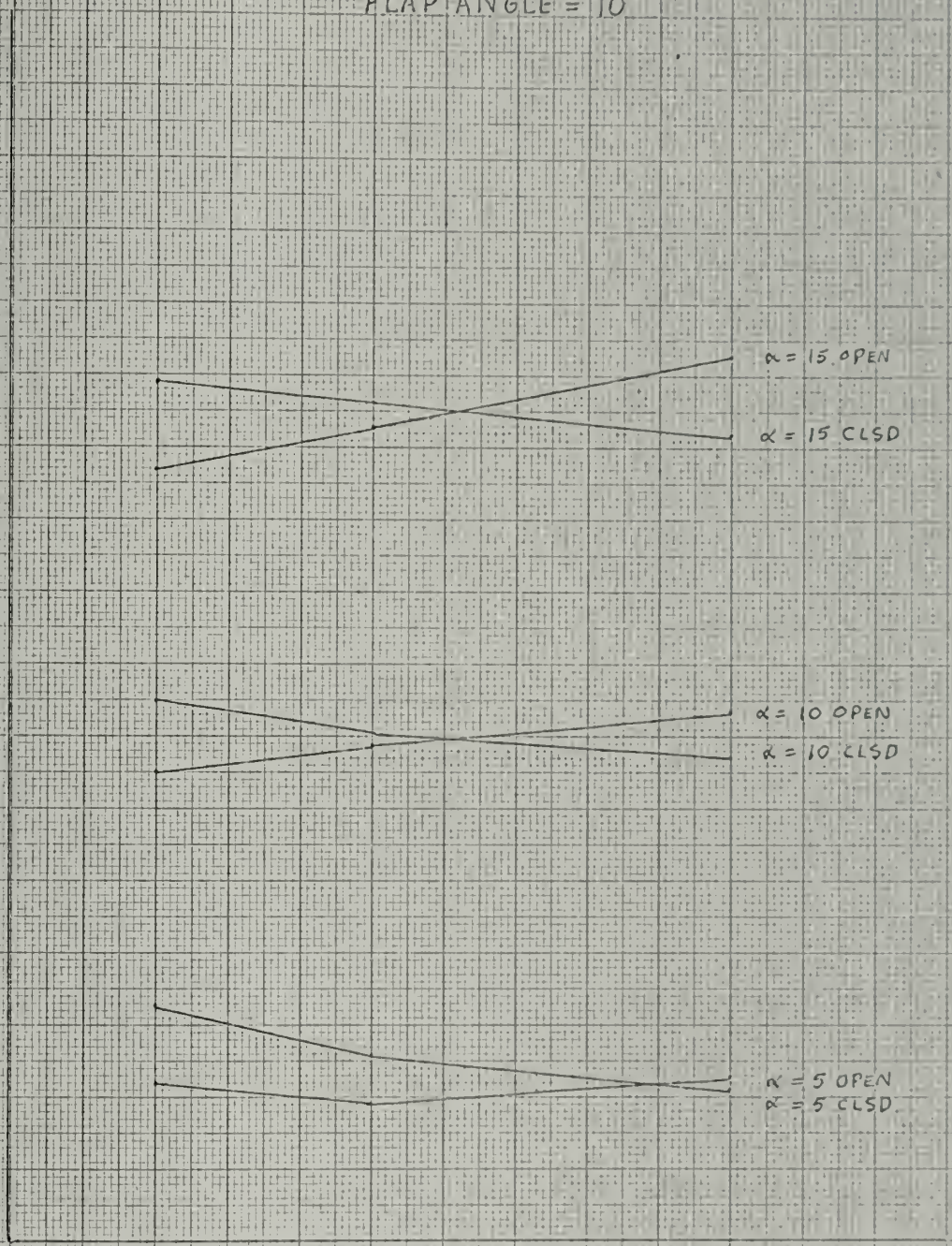
LIFT COEFFICIENT VS GAP WIDTH
FLAP ANGLE = 10
1.0
.9
.8
C_L
.7
.6
.5
.4
.3
α = 15 OPEN
α = 15 CLSD
α = 10 OPEN
α = 10 CLSD
α = 5 OPEN
α = 5 CLSD
.020
.050
.100
GAP WIDTH

Figure 30

LIFT COEFFICIENT VS GAP WIDTH
FLAP ANGLE = 15°

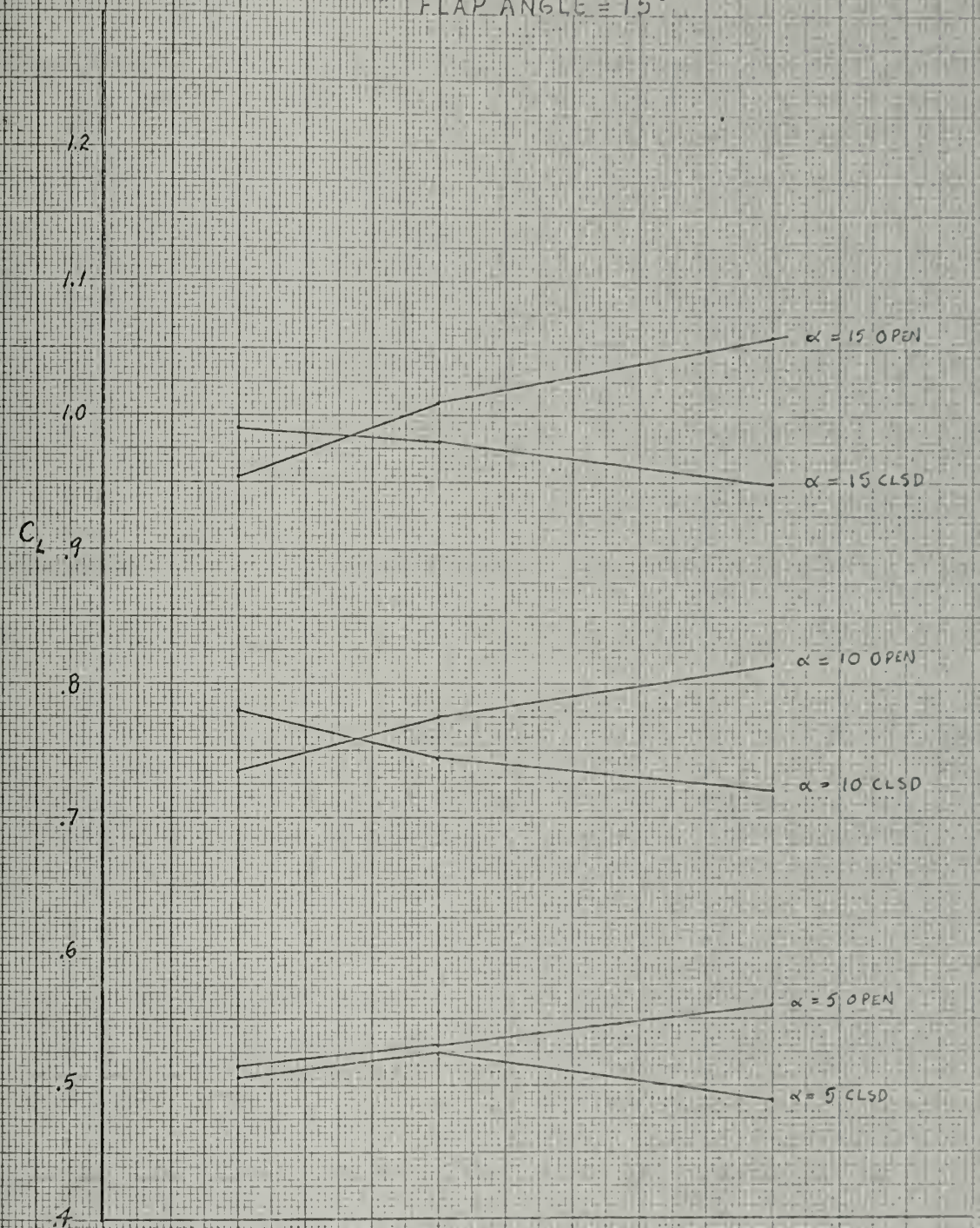

Figure 31

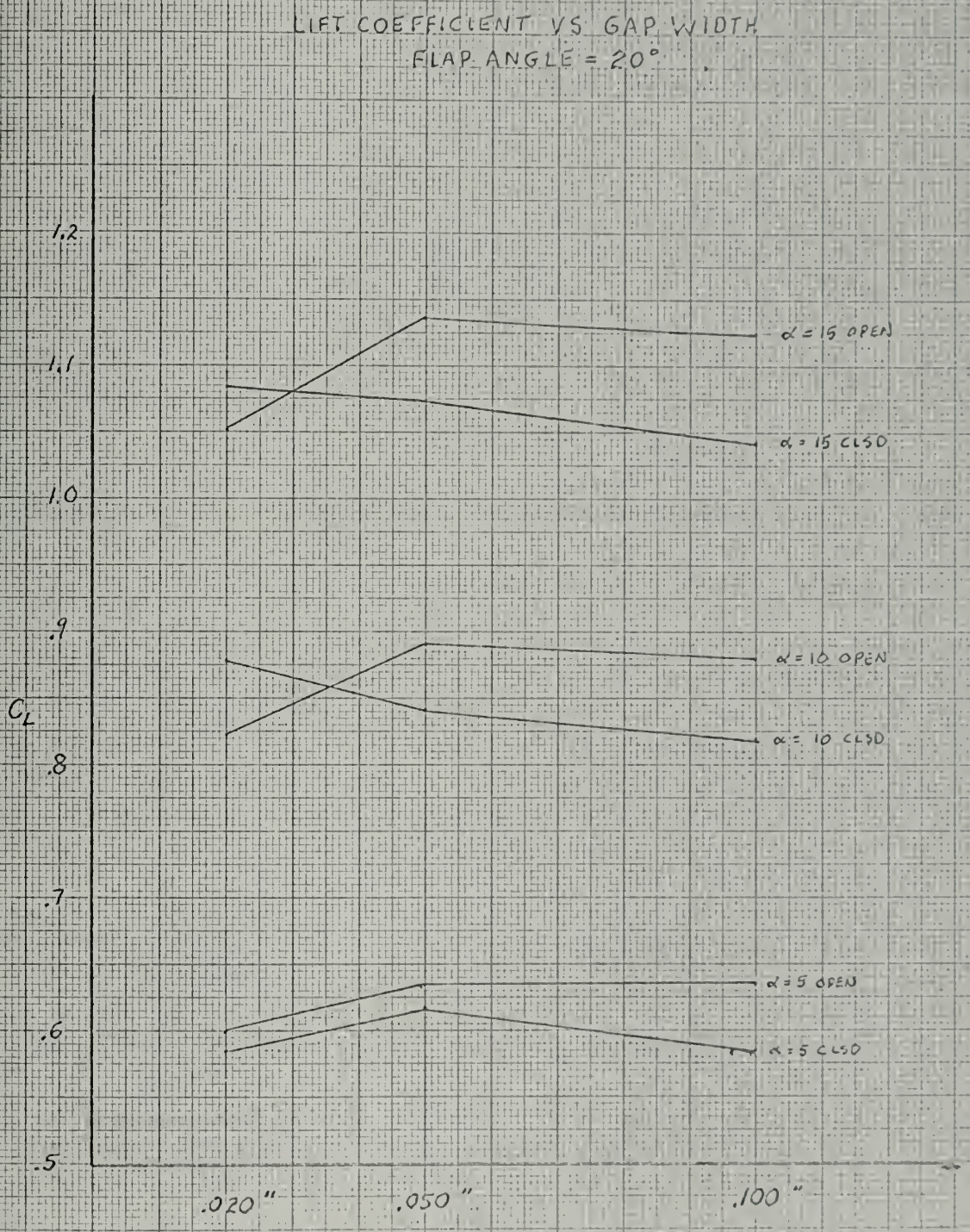
LIFT COEFFICIENT VS GAP WIDTH
FLAP ANGLE = 20°
1.2
1.1
1.0
.9
.8
.7
.6
.5
C_L
α = 15 OPEN
α = 15 CLSD
α = 10 OPEN
α = 10 CLSD
α = 5 OPEN
α = 5 CLSD
.020"
.050"
.100"
GAP WIDTH

Figure 32

$\frac{dC_L}{d\alpha}(15)$ VERSUS GAP WIDTH

α = 0 TO 15 DEGREES

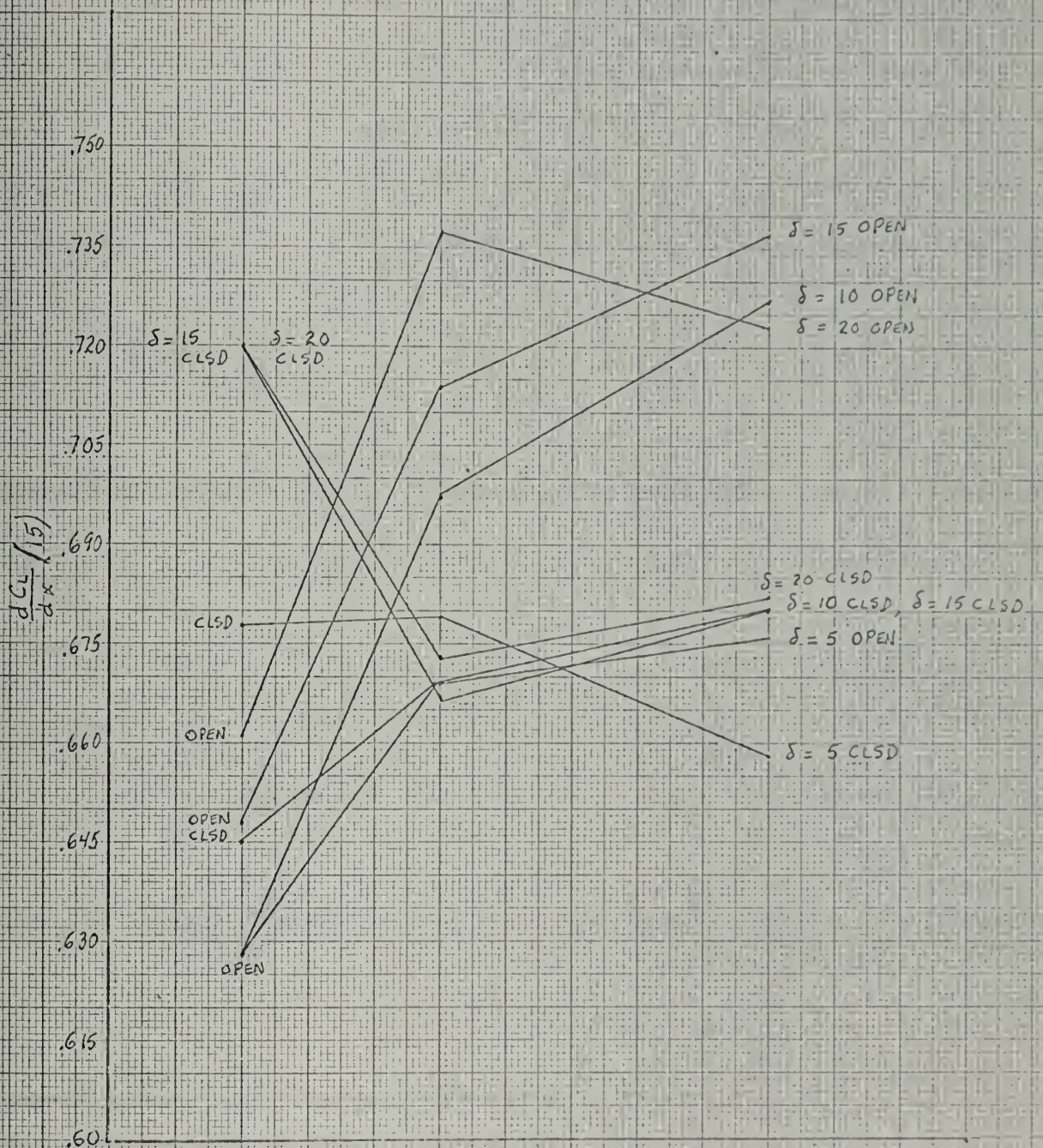

Figure 33

$\frac{dC_L}{d\delta}(\Delta\delta)$ VERSUS GAP WIDTH

$\Delta\delta$ = 0 TO 35 DEGREES

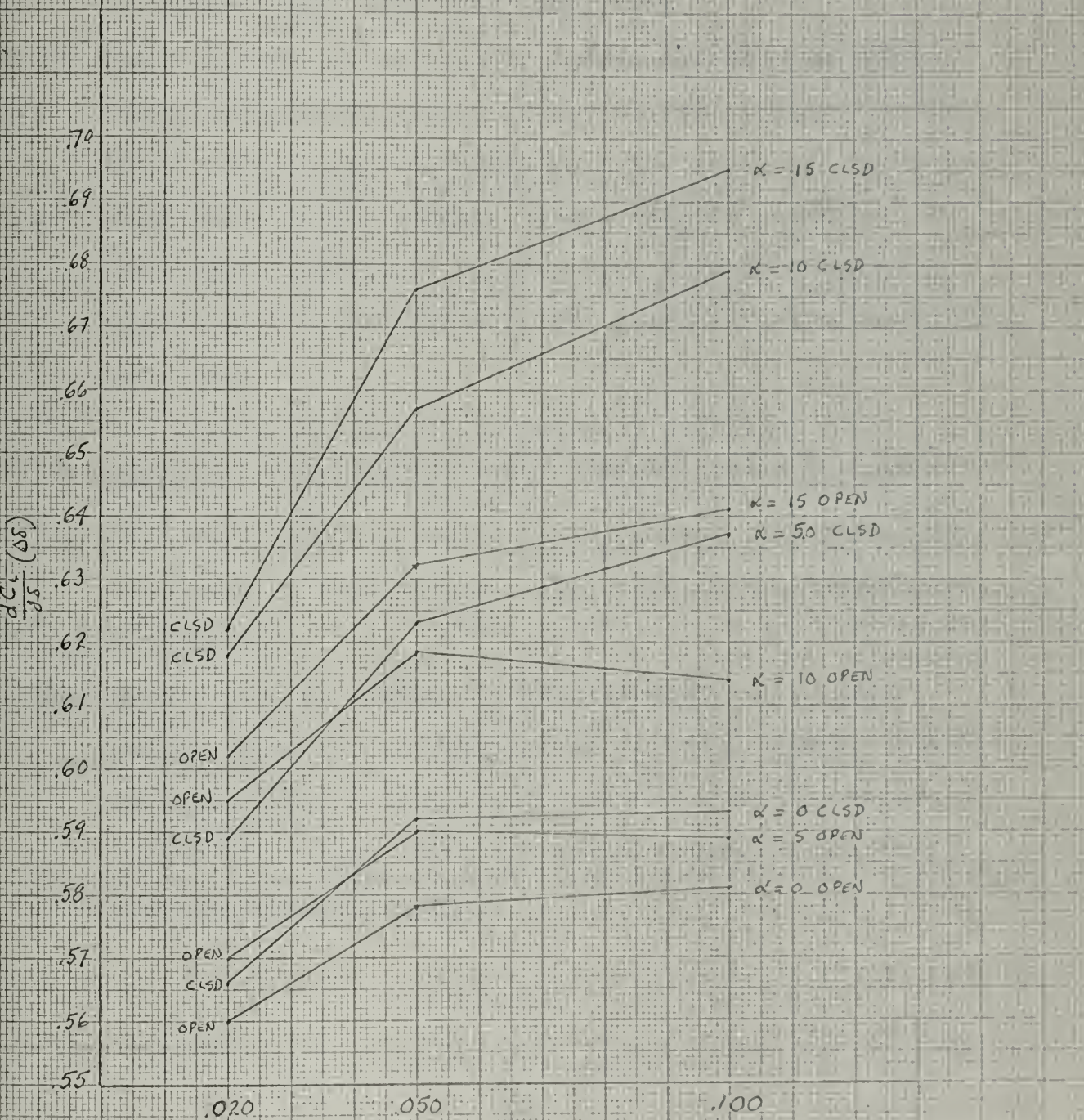

V. CONCLUSIONS

(1) The force-moment dynamometer functions properly and meets its design requirements. The design eliminates all significant load cell cross talk.

(2) The existance of an open or closed gap and gap width variation have an effect on the rudder characteristics. These effects are dependent upon the angle of attack and flap angle of the rudder. These effects could be considered negligible or important dependent upon the operational requirements of the design and the designer's judgement.

(3) The theoretical method proposed in reference 13 determines qualitative results which are in agreement with experimental results to the extent of correlation attempted in this thesis. The quantitative results are not similar.

(4) If one were to design a rudder similar to the test rudder which was to function in an alpha domain of 0 to 20 degrees and a flap angle range of 0 to 20 degrees, choice of a larger open gap would result in the best over-all characteristics.

VI. RECOMMENDATIONS

(1) More extensive output from the theoretical method of reference 13 should be generated and compared with the results of this work. The information considered was limited to that available for comparison. This was lift coefficient data at one angle of attack and flap angle.

(2) Larger gap widths than those considered in this thesis should be investigated.

(3) The effect of the gap position along the chord should be investigated.

(4) Utilizing the results of recommendations 1,2,and 3 modify the theoretical method and develop an empirically verified theory.

(5) Consider the vertical force on the rudder in future tests.

(6) Investigate the effects of gap variation on rudder flap moment.

(7) Investigate the effects of root gap variation on lift characteristics.

VII. APPENDIX

DESCRIPTION OF APPARATUS

1 Force-Moment Dynamometer

General

Prior to this experimental work a force-moment dynamometer incorporating five strain gage load cells was utilized to measure forces on hydrofoil sections. Although this device effectively measured the desired forces and moments it was plagued by motion between the force measurement planes and possessed an inability to maintain a reasonably constant measurement reference system. The result of this was an undesireable characteristic, the introduction of cross talk among the various strain gages.

In an attempt to reduce load station cross talk, and establish a reasonably fixed measurement reference system, the dynamometer utilized during this experimental investigation was constructed. This device is generally characterized by a high degree of rigidity or stiffness, and a load cell arrangement which more directly measures the forces and moments normally of concern in the testing of lifting surfaces excluding propellers.

Coordinate System, Force-Moment Sign Convention

Figure 34 illustrates the convention adopted to signify positive directions, forces and moments. Two axis systems are used throughout this investigation: instrument axis,

as depicted in figure 34, and stream axis which orients all forces and moments relative to the stream velocity in the normal aerodynamic fashion.

Load Cell Arrangement

Figure 35 illustrates the arrangement of all six load cell stations. Figure 36 illustrates the horizontal X-Z plane arrangement of three load cells mounted in the plane of the dynamometer spider. In the case of a rudder oriented perpendicular to the X-Z plane, it is possible to measure normal force, chordwise force, and yaw moment about the rudder shaft. Below are the expressions for these forces and moment:

Normal force = -C(1)*R(1)-C(2)*R(2)

Chordwise force = -C(3)*R(3)

Yaw moment = -18*C(2)*R(2)

The subscripted C refers to the calibration constant of the load cells located at the numbered stations in the horizontal plane. The subscripted R refers to the reading associated with the individual load cells at the numbered stations. The moment arm from the shaft mounting in the dynamometer spider to station 2 is 18 inches.

Figure 37 and figure 38 illustrate the vertical arrangement of three load cells normal to the X-Z plane of the dynamometer, located on a seven inch radius from the shaft mount at 120 degree positions on the dynamometer spider. In the case of a rudder it is possible to measure

Figure 34

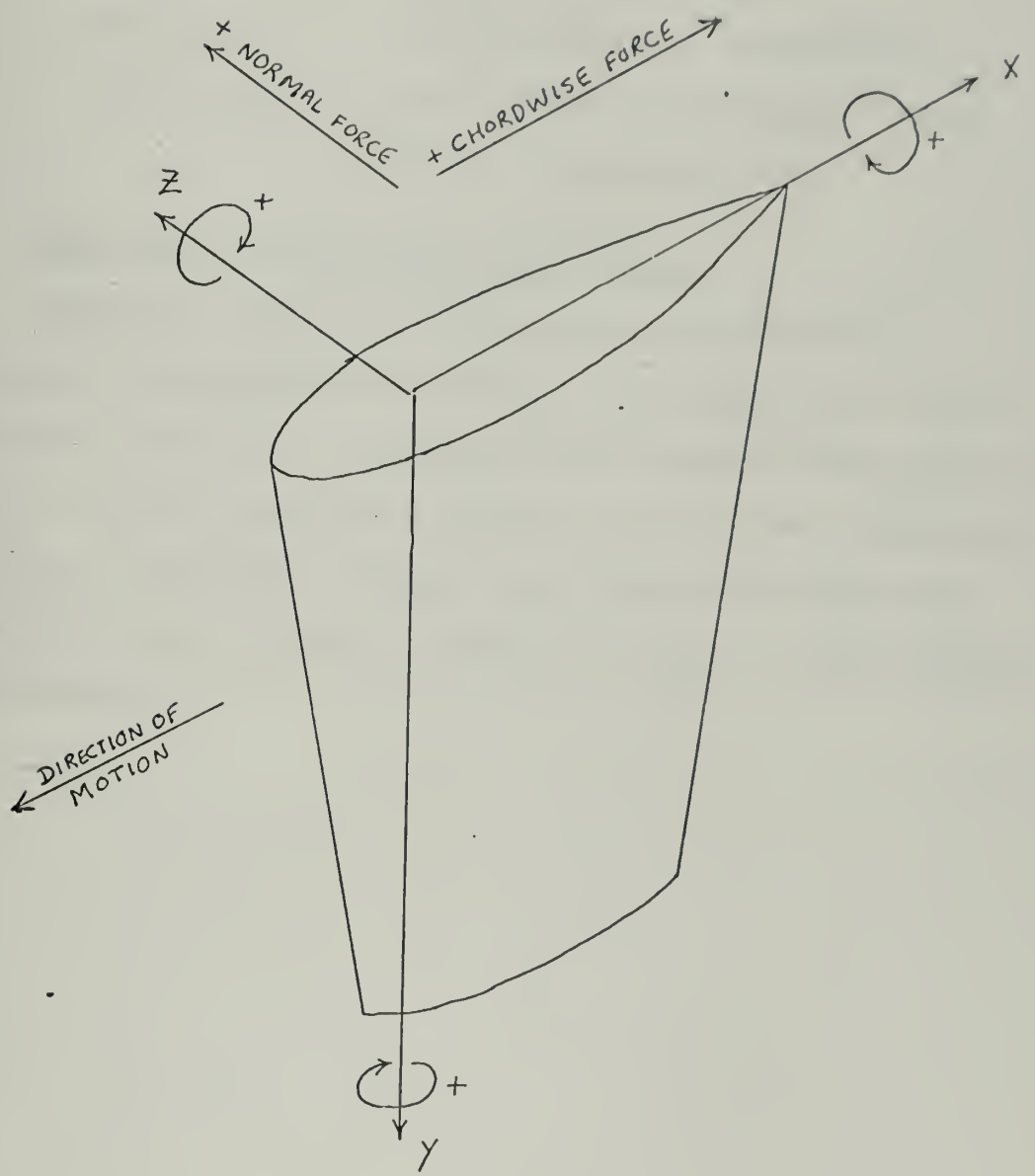

vertical force, roll and pitch moments with this arrangement. It is assumed in this investigation that the vertical force on the rudder is negligible. Listed below are expressions for the pitch and roll moments:

Pitch moment = 4.6*C(3)*R(3)-10.5*C(6)*R(6)

Roll moment = 4.6*(C(1)*R(1)+C(2)*R(2))-12.124*(
C(4)*R(4)+C(6)*R(6)/2)

II Load Cells and Recording Instruments

Stations 1,4, and 5 are configured with 500 lb. capacity Lebow wheatstone bridge strain gage load cells. Stations 3 and 6 are configured with similar Lebow load cells with a 200 lb. capacity. Station 2 also uses a Lebow cell of 50 lb. capacity. Signals from these load cells are converted into a digital reading by means of Lebow Digital Indicators.

Figure 35

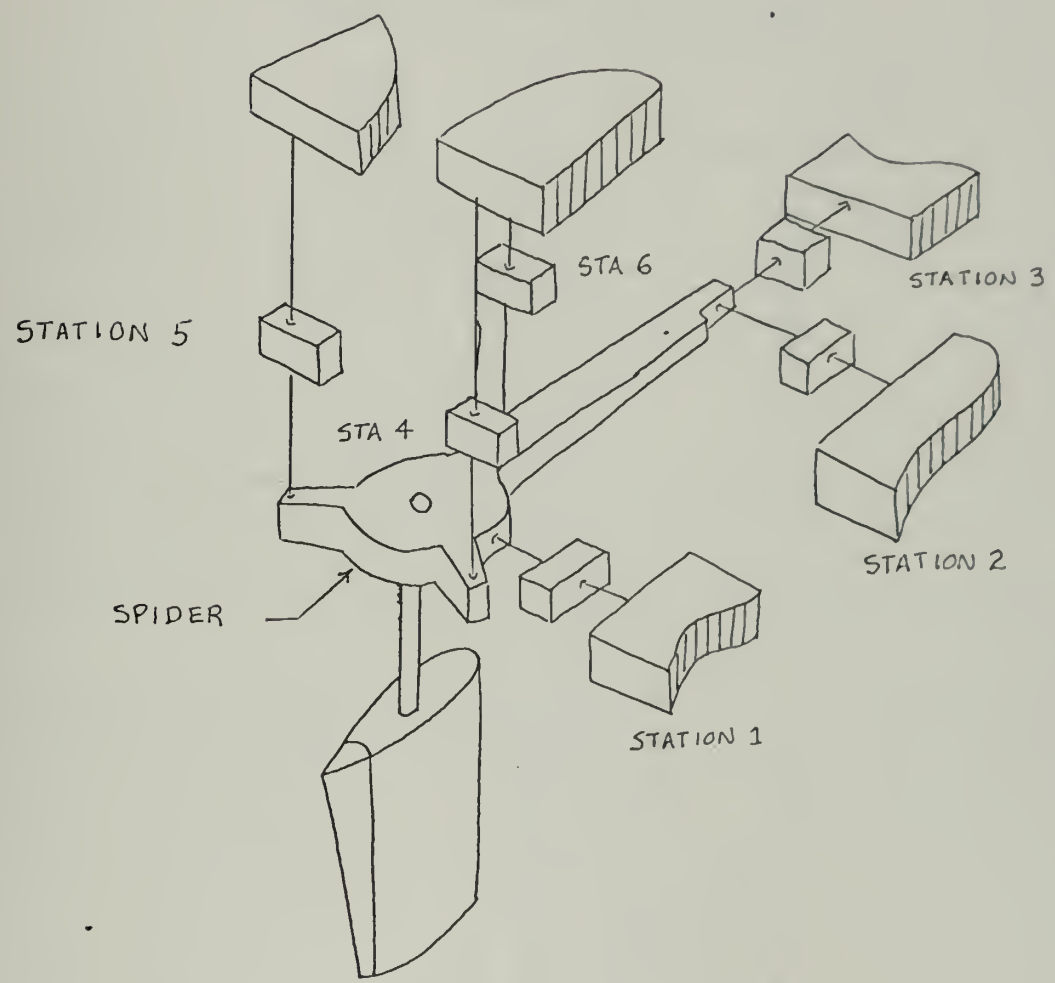

Figure 36

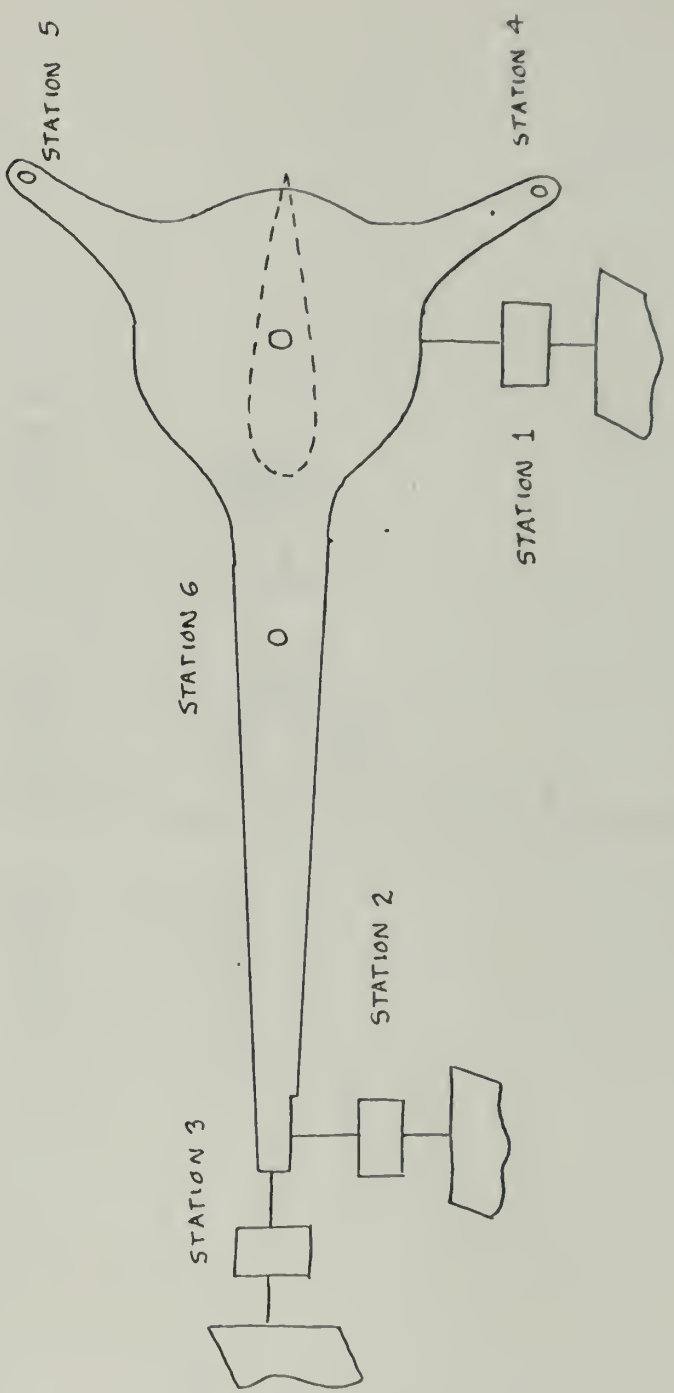

Figure 37

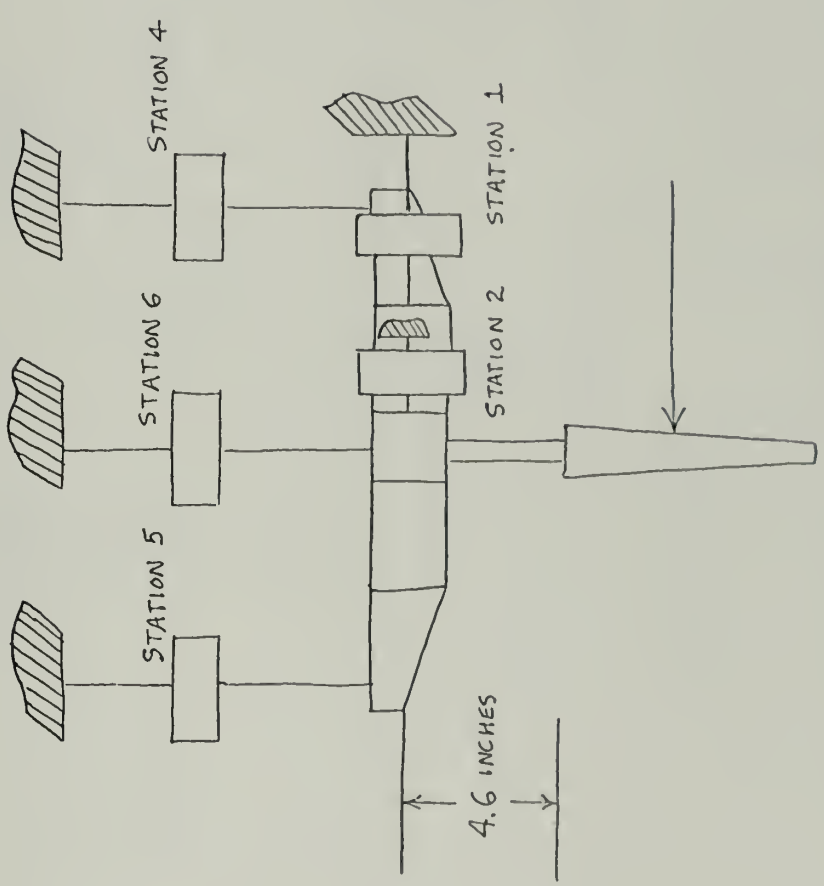

Figure 38

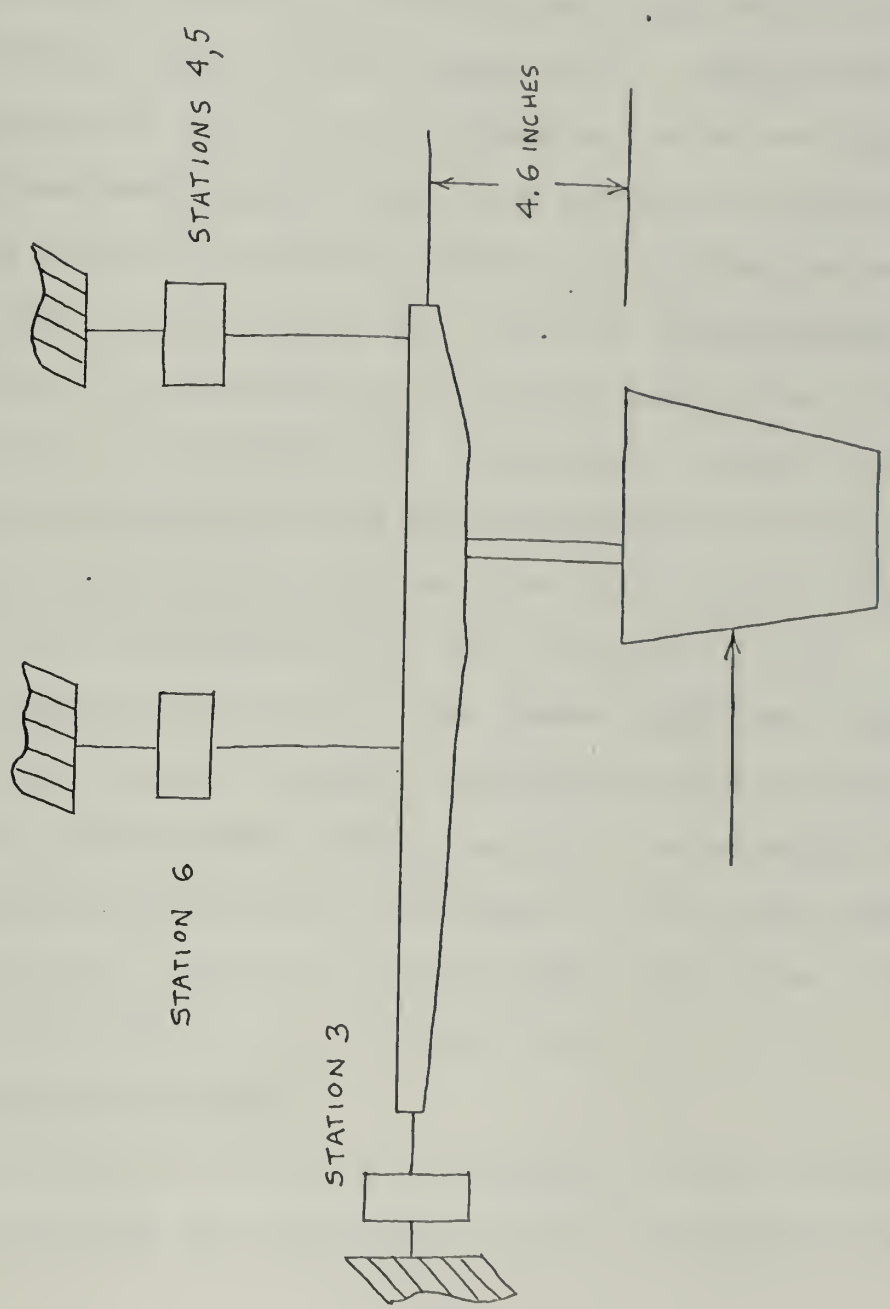

III System Calibration

Load Cell

The entire system, dynamometer, load cells, cabling and digital indicators is calibrated as a unit. The process consists of recording indicator readings associated with known weights placed on a calibration shaft or T-bar which is mounted in place of the rudder shaft. Calibration constants with units of lbs. force per count are developed from these measurements, the known position of the weight, and the load cell geometry. Using the calibration shaft and placing weights along its length at predetermined positions it is possible to calibrate load cells at stations 1, 3, and 4, by rotating the dynamometer through 90 degrees while it is mounted on its side in the water tunnel. Similarly calibration constants for load cells at stations 2 and 6 are determined using the calibration T-bar. This T-bar geometry introduces a yaw moment dependent upon the dynamometer angular position in addition to the other forces roll and pitch moments associated with the straight shaft. The calibration constants determined by the above methods are: cell one, .0970; cell two, .0558; cell three, .2374; cell four, .1013; and cell six, .2831.

Rudder Shaft Twist

In order to determine the amount of twist of the rudder when acted upon by a twisting moment, a contoured moment arm

is fitted to the rudder mounted in the dynamometer. By means of a WWII gunner's quadrant the angular rotation of the rudder is determined for the applied weight at a known position from the rudder shaft. The value determined is 1/733.3 degrees per inch-lb.

DATA REDUCTION COMPUTER PROGRAM

The data accumulated during the experiments, certain rudder constants, and environmental conditions are utilized as input to the program. The computer program resolves the input into the following output:

1. Forces and moments relative to the dynamometer coordinate system at a particular dynamometer angle.

2. Forces and moments relative to the stream coordinate system at a particular angle of attack.

3. Coefficients of lift, drag, rudder moment, flap moment, and center of pressure coefficients for lift and drag at a particular angle of attack.

Each set of output is associated with a specific flap angle. In this investigation flap angle settings from 0 to 35 degrees at 5 degree intervals were used. Therefore each rudder is described by eight sets of data.

```
C     NEW DYNAMOMETER//RUDDER DATA REDUCTION PROGRAM   KERWIN/CHAMPLAIN 3/71
      INTEGER RS,S,BLANK
      DIMENSION IDENT(18),ZM(2),ZI(6,2,2),ZF(2),NTAP(20),NFLD(20),ANUM(2
     10),ANGL(20),S(20,6),R(20,7),DZI(6,2),FL(20),FD(20),FY(20),FR(20),F
     2F(20),FP(20),SI(20),CO(20),SL(20),SD(20),SR(20),SP(20),CL(20),CD(2
     30),CY(20),CR(20),CP(20),CF(20),VC(5),VE(5),FM(2),C(6)
      DATA VC/4.11447,2.60088,0.9016,0.6214,4.7381/,VE/.49353,.5,.4724,0
     1.50638,.5/,RS/'R'/,BLANK/' '/
    1 READ(5,103)(IDENT(N),N=1,18)
  103 FORMAT(18A4)
      READ(5,100) DF,NRT,NTT,AREA,SPAN,AC,XAC,ZAC,FMC
  100 FORMAT(F5.1,I5,I6,F10.2,F9.1,F9.3,F9.3,F18.2,F9.2)
      IF(AREA.LE.0) GO TO 99
      RHO=1.9574-0.00028*NTT
      SCALE=1.000952-13.3E-6*NRT
      FM(1)=1.4875-.00071*NRT
      FM(2)=24.5054-.00236*NRT
      WRITE(6,200)(IDENT(N),N=1,18)
  200 FORMAT('1'17X'FLAPPED RUDDER INPUT DATA'/18A4/3X'DF'3X'TR'4X'TT'5X
     1'AREA'6X'SPAN'4X'C-MAC'4X'X-MAC'14X'ZAC'6X'FMC')
      WRITE(6,100) DF,NRT,NTT,AREA,SPAN,AC,XAC,ZAC,FMC
      READ(5,101)(ZM(K),((ZI(M,L,K),L=1,2),M=1,6),ZF(K),K=1,2)
  101 FORMAT(F5.0,12X,F5.0,F4.0,F5.0,F4.0,F5.0,F4.0,F5.0,F4.0,F5.0,F4.0,
     1F5.0,F4.0,F9.0)
      WRITE(6,201)
  201 FORMAT('     ZERO READINGS BEFORE AND AFTER'/' VEL 1-N   1-R   2-N
     1  2-R   3-N   3-R   4-N   4-R   5-N   5-R   6-N   6-R   FLAP')
      WRITE(6,204)(ZM(K),((ZI(M,L,K),L=1,2),M=1,6),ZF(K),K=1,2)
  204 FORMAT(2(F3.0,4(2X,F4.0),2(1X,F4.0),6(2X,F4.0),1X,F6.0/))
      WRITE(6,202)
  202 FORMAT(//'     INPUT DATA AS RECORDED'/'  TF  VEL  ANGLE   S    1
     1 S    2   S    3   S    4   S    5   S    6      FLAP')
      DO 2 J=1,20
      JT=J-1
      READ(5,102) NTAP(J),NFLD(J),ANUM(J),ANGL(J),(S(J,M),R(J,M),M=1,6),
     1R(J,7)
```

```
102  FORMAT(I4,I1,F5.0,F6.1,3X,A1,F8.2,A1,F8.2,A1,F8.2,A1,F8.2,A1,F8.2,
    1A1,F8.2,F7.0)
     IF(ANOM(J).LE.0.0) GO TO 3
2    WRITE(6,203) NTAP(J),NFLD(J),ANOM(J),ANGL(J),(S(J,M),R(J,M),M=1,6)
    1,R(J,7)
203  FORMAT(I3,I1,F6.0,F6.1,3X,6(A1,F6.0,2X),F7.0)
     GO TO 99
3    BUG=1.0/(JT-1)
     DZM=(ZM(2)-ZM(1))*BUG
     DO 4 M=1,6
     DO 4 L=1,2
4    DZI(M,L)=(ZI(M,L,2)-ZI(M,L,1))*BUG
     DZF=(ZF(2)-ZF(1))*BUG
     DO 5 J=1,JT
     IF(J.EQ.1) GO TO 6
     IF(NTAP(J).EQ.0) NTAP(J)=NTAP(J-1)
     IF(NFLD(J).EQ.0) NFLD(J)=NFLD(J-1)
6    BUG=J-1
     ANOM(J)=ANOM(J)-ZM(1)-BUG*DZM
     RAT=(ANGL(J)-101.0)*0.0174532
     SI(J)=SIN(RAT)
     CO(J)=COS(RAT)
     ANGL(J)=ANGL(J)-ZAC
     DO 7 M=1,6
     IF(S(J,M).EQ.BLANK) S(J,M)=S(J-1,M)
     IF(S(J,M).EQ.RS) GO TO 8
     R(J,M)=R(J,M)-ZI(M,1,1)-BUG*DZI(M,1)
     GO TO 7
8    R(J,M)=-R(J,M)+ZI(M,2,1)+BUG*DZI(M,2)
7    CONTINUE
5    R(J,7)=R(J,7)-ZF(1)-BUG*DZF
     WRITE(6,205)(NTAP(J),NFLD(J),ANOM(J),ANGL(J),(R(J,M),M=1,6),R(J,7)
    1,J=1,JT)
205  FORMAT(//'     INPUT DATA CORRECTED FOR ZERO READINGS AND SIGNS'/(I
    13,I1,F6.0,F6.1,3X,6F9.2,F7.0))
     WRITE(6,207)
```

```
207  FORMAT(//'     FORCES IN POUNDS AND IN-POUNDS  INSTR AXES,STREAM')
     C(1)=.0970
     C(2)=.0568
     C(3)=.2374
     C(4)=.1013
     C(6)=.2831
     DO 9 J=1,JT
     FL(J)=-C(1)*R(J,1)-C(2)*R(J,2)
     FD(J)=-C(3)*R(J,3)
     FY(J)=-C(2)*18*R(J,2)
     FP(J)=4.6*C(3)*R(J,3)-10.5*C(6)*R(J,6)
     FR(J)=4.6*(C(1)*R(J,1)+C(2)*R(J,2))-12.124*(C(4)*R(J,4)+C(6)*R(J,6
    1)/2.0)
     FF(J)=R(J,7)/FMC
     ANGL(J)=ANGL(J)+FY(J)/733.3
     SL(J)=FL(J)*CC(J)-FD(J)*SI(J)
     SD(J)=FD(J)*CC(J)+FL(J)*SI(J)
     SR(J)=FR(J)*CC(J)-FP(J)*SI(J)
     SP(J)=FP(J)*CC(J)+FR(J)*SI(J)
     I=NTAP(J)
     IF(I.LT.1.OR.I.GT.5) GO TO 99
     K=NFLD(J)
     IF(K.LT.1.OR.K.GT.2) GO TO 99
     BUG=VE(I)
     V=(ANOM(J)*FM(K)*SCALE/(VC(I)*RHO))**BUG
     WRITE(6,206) ANGL(J),FL(J),FD(J),FY(J),FR(J),FP(J),FF(J),SL(J),SD(
    1J),SR(J),SP(J),V
206  FORMAT(12F9.2)
     RVS=0.5*RHO*AREA*V**2/144.0
     CL(J)=SL(J)/RVS
     CD(J)=SD(J)/RVS
     CY(J)=(FY(J)+FL(J)*XAC)/RVS/AC
     CR(J)=(SR(J)/SL(J))/SPAN
     CP(J)=(SP(J)/SD(J))/SPAN
9    CF(J)=FF(J)/RVS/AC
     WRITE(6,208)(IDENT(N),N=1,18)
```

```
208  FORMAT('1  **FLAPPED RUDDER DATA IN NON-DIMENSIONAL FORM**'//3X18A
    14//'   ALPHA     CL     CD      CM      CPL     CPD     CMF')
     WRITE(6,209)(ANGL(J),CL(J),CD(J),CY(J),CR(J),CP(J),CF(J),J=1,JT)
209  FORMAT(F8.2,6F7.3)'
     DO 15 J=1,JT
     ANGL(J)=ANGL(J)+1.404*CL(J)
15   CD(J)=CD(J)+0.0244*CL(J)**2
     WRITE(6,211)
211  FORMAT(///'    ABOVE DATA CORRECTED FOR TUNNEL INTERFERENCE'
    1 //'   ALPHA     CL     CD      CM      CPL     CPD     CMF')
     WRITE(6,209)(ANGL(J),CL(J),CD(J),CY(J),CR(J),CP(J),CF(J),J=1,JT)
     ANGL(JT+1)=0.0
     CL(JT+1)=0.0
     CD(JT+1)=0.0
     CY(JT+1)=0.0
     CF(JT+1)=0.0
     CR(JT+1)=0.0
     CP(JT+1)=0.0
     WRITE(7,210) DF
210  FORMAT(10F8.3)
     JA=1
14   JB=JA+1
     WRITE(7,210)(ANGL(J),CL(J),CD(J),CY(J),CF(J),CR(J),CP(J),J=JA,JB)
     JA=JA+2
     IF(JA.LE.JT) GO TO 14
     GO TO 1
99   STOP
     END
```

DEFINITION OF VARIABLES

IDENT = Rudder description

ZM = Velocity manometer zero reading

ZI = Digital indicator zero reading

ZF = Flap indicator zero reading

NTAP = Velocity manometer valve arrangement code

NFLD = Manometer fluid code

ANOM = Manometer reading in mm

ANGL = Dynamometer angle or angle of attack if corrected for the angle of zero lift

S = Sign signifying the quadrant in which the Lebow indicator is operating

R = Reading of the digital indicator

FL = Normal force, instrument axis

FD = Chordwise force, instrument axis

FY = Yaw moment, instrument and stream axes

FR = Roll moment, instrument axis

FP = Pitch moment, instrument axis

FF = Flap moment, instrument and stream axis

SL = lift force

SD = Drag force

SR = Roll moment, stream axis

SP = Pitch moment, stream axis

C = Load cell calibration constant

CL,CD,CY,CR,CP,CF = Coefficients of lift force, drag force, yaw, roll, pitch, and flap moment

CURVE PLOTTING COMPUTER PROGRAM

The experimental results are represented by graphic plots. The plotting was accomplished by a computer program and the S-C 4020 Computer Recorder manufactured by Stromberg-Carlson. The input for this program is the output of the data reduction program, coefficients at angle of attack with the parameter flap angle. The basic features of the program are a 5 point 3 degree curve smoothing method outlined in reference 6 incorporated in a smoothing subroutine which smooths the points both vertically at constant angle of attack, and horizontally at constant flap angle; a Lagrange method interpolation subroutine, and the main program directing the plot set up and execution. The output is a printed set of interpolated lift, drag, rudder moment, flap moment, and center of pressure coefficients versus angle of attack at each flap angle, and a graphical presentation of this data in the form of a family of curves similar to those encountered in aerodynamic publications.

```
C      *** PLOT FLAPPED RUDDER DATA *** JANUARY 1971
       DIMENSION LABEL(18),AFLP(9),ALPHA(14,9),CL(61,9),CD(61,9),CM(61,9)
      1,CMF(61,9),SCL(14,9),SVCL(14,9),PLOTA(61),Y(8,13),CF(36,13),PLOTF(
      236),COFF(61,9),CR(61,9),CP(61,9)
       INTEGER ABLM
       EXTERNAL TABL1V,TABL2V
       CALL IDFRMV('MITMARHYDLAB','N4','MITRUDPL')
       CALL RITSTV(13,18,TABL1V)
       CALL CHSIZV(2,2)
    1  READ(5,100) NSTOP
  100  FORMAT(I1)
       IF(NSTOP.EQ.0) GO TO 99
       NCT=0
       READ(5,101)(LABEL(N),N=1,18)
  101  FORMAT(18A4)
       DO 2 M=1,9
       READ(5,102) AFLP(M)
  102  FORMAT(10F8.3)
       NA=1
    3  NB=NA+1
       READ(5,102)(ALPHA(N,M),CL(N,M),CD(N,M),CM(N,M),CMF(N,M),CR(N,M),CP
      1(N,M),N=NA,NB)
       NA=NA+2
       IF(NA.LE.13) GO TO 3
    2  CONTINUE
    7  NCT=NCT+1
       IF(NCT.EQ.4) GO TO 7
       IF(NCT.EQ.7) GO TO 1
       IF(NCT.EQ.5) GO TO 40
       IF(NCT.EQ.6) GO TO 40
       IF(NCT.GT.1) GO TO 39
       ORMN=-1.2
       ORMX=1.8
       ORDV=0.2
       ABLM=324
       DO 55 J=1,8
```

```
      DO 55 I=1,13
55    COEF(I,J)=CL(I,J)
      GO TO 56
39    IF(NCT-3) 41,42,43
41    ORMN=0.0
      ORMX=1.2
      ORDV=0.1
      ABLM=92
      GO TO 40
42    ORMN=-0.35
      ORMX=0.15
      ORDV=0.05
      GO TO 40
43    ORMN=-0.15
      ORMX=0.10
      ORDV=0.025
      GO TO 40
40    DO 8 MM=1,8
      DO 8 NN=1,13
      IF(NCT.EQ.5) GO TO 72
      IF(NCT.EQ.6) GO TO 73
      IF(NCT-3) 10,13,19
10    COEF(NN,MM)=CD(NN,MM)
      GO TO 8
13    COEF(NN,MM)=CM(NN,MM)
      GO TO 8
19    COEF(NN,MM)=CMF(NN,MM)
      GO TO 8
72    COEF(NN,MM)=CR(NN,MM)
      GO TO 8
73    COEF(NN,MM)=CP(NN,MM)
      GO TO 8
8     CONTINUE
56    DO 61 M=1,8
      DO 61 N=1,6
      K=14-N
```

```
      IF(NCT.GT.1) GO TO 57
      BUG=ALPHA(N,M)
      ALPHA(N,M)=ALPHA(K,M)
      ALPHA(K,M)=BUG
   57 BUG=COEF(N,M)
      COEF(N,M)=COEF(K,M)
      COEF(K,M)=BUG
   61 CONTINUE
      CALL SMOOTH(COEF,SCL,SVCL)
      DO 14 N=1,61
      PLOTA(N)=N-31
      DO 14 M=1,8
   14 COEF(N,M)=FILLIN(PLOTA(N),ALPHA(1,M),SVCL(1,M),13)
      IF(NCT.GT.2) GO TO 80
      IF(NCT.GT.1) GO TO 81
      DO 84 N=1,30
      MONK=31-N
      MOLE=N+31
      BUG=0.5*(COEF(MOLE,1)+COEF(MONK,1))
      DO 82 M=1,8
      COEF(MOLE,M)=COEF(MOLE,M)-BUG
   82 COEF(MONK,M)=COEF(MONK,M)-BUG
   84 CONTINUE
      GO TO 80
   81 DO 83 N=1,30
      MONK=31-N
      MOLE=N+31
      BUG=0.5*(COEF(MOLE,1)-COEF(MONK,1))
      DO 85 M=1,8
      COEF(MOLE,M)=COEF(MOLE,M)-BUG
   85 COEF(MONK,M)=COEF(MONK,M)+BUG
   83 CONTINUE
   80 WRITE(6,104)(PLOTA(N),(COEF(N,M),M=1,8),N=1,61)
  104 FORMAT(9F12.3)
      IF(NCT.GT.1)  GO TO 60
      K=0
```

```
      IF(NCT.EQ.5) GO TO 76
      IF(NCT-3) 25,26,27
25    CALL RITE2V(9.350,1023.180,4.21.-1.21HDRAG COEFFICIENT   CD,NUT)
      GO TO 22
26    CALL RITE2V(9.350,1023.180,4.23.-1.23HRUDDER MOMENT COEF   CM,NUT)
      GO TO 22
27    CALL RITE2V(9.350,1023.180,4.22.-1.22HFLAP MOMENT COEF   CMF,NUT)
      GO TO 22
76    CALL RITE2V(9.635,1023.180,4.21.-1.21HROLL PRESS COEF   CPL,NUT)
      ORMN=0.0
      ORMX=1.0
      GO TO 22
77    CALL RITE2V(9.100,1023.180,4.21.-1.22HPITCH PRESS COEF   CPD,NUT)
      ORMN=0.0
      ORMX=1.0
      GO TO 22
22    NXL=IXV(-30.0)
      NXR=IXV(30.0)
      NYB=IYV(ORMN)
      NYT=IYV(ORMX)
      DO 4 INK=1,10
      CALL LINEV(NXL,NYB,NXR,NYB)
      CALL LINEV(NXR,NYB,NXR,NYT)
      CALL LINEV(NXR,NYT,NXL,NYT)
4     CALL LINEV(NXL,NYT,NXL,NYB)
      INK=4
      DO 5 M=1,8
      INK=INK-1
      IF(INK.EQ.0) INK=3
      NXL=IXV(PLOTA(1))
      NYB=IYV(COEF(1,M))
      NIXON=1
      DO 6 N=1,60
      NXR=IXV(PLOTA(N+1))
      NYT=IYV(COEF(N+1,M))
      MDASH=INK/NIXON
```

```
      IF(YDASH.GT.0) GO TO 31
      NIXON=1
      GO TO 32
   31 DO 11 I=1,8
   11 CALL LINEV(NXL,NYB,NXR,NYT)
      NIXON=NIXON+1
      IF(NIXON.GT.3) NIXON=1
   32 NXL=NXP
    6 NYB=NYT
    5 CONTINUE
      WRITE(6,103)
  103 FORMAT('   PLOT COMPLETED')
      IF(NCT.EQ.1) GO TO 35
      GO TO 7
C     PLOTTING AFLP VS CL CONSTANT ALPHA
   35 CALL SETMIV(671,68,24,45)
      CALL GRID1V(2.0,0.35,0.,-1.2,1.8,5.0,0.2,0.0,-2.0,0.4,0)
      NXL=IXV(0.0)
      NXR=IXV(35.0)
      NYB=IYV(-1.2)
      NYT=IYV(1.8)
      DO 18 INK=1,10
      CALL LINEV(NXL,NYB,NXR,NYB)
      CALL LINEV(NXR,NYB,NXR,NYT)
      CALL LINEV(NXR,NYT,NXL,NYT)
   18 CALL LINEV(NXL,NYT,NXL,NYB)
      NIXON=1
      MOUSE=1
      INK=4
      DO 23 N=1,13
      INK=INK-1
      IF(INK.EQ.0) INK=3
      NXL=IXV(PLOTF(1))
      NYB=IYV(CF(1,N))
      DO 29 M=2,36
      NXR=IXV(PLOTF(M))
```

```
      NYT=IYV(CF(M,N))
      MDASH=INK/NIXON
      IF(MDASH.GT.0) GO TO 33
      NIXON=1
      GO TO 34
33    DO 3) I=1,8
3     CALL LINEV(NXL,NYB,NXR,NYT)
      NIXON=NIXON+1
      IF(NIXON.GT.3) NIXON=1
34    NXL=NXR
29    NYB=NYT
      MOUSE=MOUSE+1
23    CONTINUE
      WRITE(6,103)
      GO TO 7
99    CALL PLTND
      STOP
      END
```

```
      SUBROUTINE SMOOTH(CL,SCL,SVCL)
      DIMENSION CL(61,9),SCL(14,9),SVCL(14,9)
C     SMOOTHING DATA 3 DEGREE 5 POINT
C     SMOOTHING END POINTS
      DO 12 M=1,3
      SCL(1,M)=(69.0*CL(1,M)+4.0*CL(2,M)-6.0*CL(3,M)+4.0*CL(4,M)-CL(5,M)
     1)/70.0
      SCL(2,M)=(2.0*CL(1,M)+27.0*CL(2,M)+12.0*CL(3,M)-8.0*CL(4,M)+2.0*CL
     1(5,M))/35.0
      SCL(13,M)=(69.0*CL(13,M)+4.0*CL(12,M)-6.0*CL(11,M)+4.0*CL(10,M)-CL
     1(9,M))/70.0
      SCL(12,M)=(2.0*CL(13,M)+27.0*CL(12,M)+12.0*CL(11,M)-8.0*CL(10,M)+2
     1.0*CL(9,M))/35.0
C     SMOOTHING INTERMEDIATE POINTS
      DO 12 N=3,11
   12 SCL(N,M)=(-3.0*CL(N-2,M)+12.0*CL(N-1,M)+17.0*CL(N,M)+12.0*CL(N+1,M
     1)-3.0*CL(N+2,M))/35.0
C     SMOOTHING VERTICALLY CONSTANT ALPHA
      DO 15 N=1,13
      SVCL(N,1)=(69.0*SCL(N,1)+4.0*SCL(N,2)-6.0*SCL(N,3)+4.0*SCL(N,4)-SC
     1L(N,5))/70.0
      SVCL(N,2)=(2.0*SCL(N,1)+27.0*SCL(N,2)+12.0*SCL(N,3)-8.0*SCL(N,4)+2
     1.0*SCL(N,5))/35.0
      SVCL(N,8)=(69.0*SCL(N,8)+4.0*SCL(N,7)-6.0*SCL(N,6)+4.0*SCL(N,5)-SC
     1L(N,4))/70.0
      SVCL(N,7)=(2.0*SCL(N,8)+27.0*SCL(N,7)+12.0*SCL(N,6)-8.0*SCL(N,4))/
     135.0
      DO 15 M=3,6
   15 SVCL(N,M)=(-3.0*SCL(N,M-2)+12.0*SCL(N,M-1)+17.0*SCL(N,M)+12.0*SCL(
     1N,M+1)-3.0*SCL(N,M+2))/35.0
      RETURN
      END
```

```
      FUNCTION FILLIN(X,AB,OR,NO)
      DIMENSION AB(1),OR(1)
      ANTRA(X1,X2,X3,X,Y1,Y2,Y3)=Y1*(X-X2)*(X-X3)/((X1-X2)*(X1-X3))+
     1 Y2*(X-X1)*(X-X3)/((X2-X1)*(X2-X3))+Y3*(X-X1)*(X-X2)/((X3-X1)*
2    2 (X3-X2))
      IF(X-AB(1)) 1,3,2
3     Y=OR(1)
      GO TO 99
1     Y=ANTRA(AB(1),AB(2),AB(3),X,OR(1),OR(2),OR(3))
      GO TO 99
2     IF(X-AB(2)) 1,6,5
6     Y=OR(2)
      GO TO 99
5     DO 7 I=3,NO
      M=I
      IF(X-AB(I)) 8,9,7
9     Y=OR(I)
      GO TO 99
7     CONTINUE
8     Y=ANTRA(AB(M-2),AB(M-1),AB(M),X,OR(M-2),OR(M-1),OR(M))
99    FILLIN=Y
      RETURN
      END
```

VIII. REFERENCES

(1) Abbott, I.H., and VonDoenhoff, A.E., Theory of Wing Sections, New York, Dover Publications, 1959

(2) Comstock, J,P., Principles of Naval Architecture, Chapter VIII, New York, The Society of Naval Architects and Marine Engineers, 1967

(3) Falkner, V.M., "The Calculation of Aerodynamic Loading on Surfaces of Any Shape", A.R.C. Technical Reports R&M No. 1910

(4) Falkner, V.M., "The Solution of Lifting-Plane Problems by Vortex-Lattice Method", A.R.C. Technical Reports R&M No. 2591, 1953

(5) Glauert, H., The Elements of Aerofoil and Airscrew Theory, Cambridge, University Press, 1959

(6) Hildebrand, F.B., Introduction to Numerical Analysis, New York, McGraw Hill, 1956

(7) Lamb, H., Hydrodynamics, New York, Dover Publications, 1945

(8) McCracken, D.D., A Guide To Fortran Programming, New York, Wiley, 1963

(9) Prandtl, L., Applied Hydro-And Aeromechanics, New York, Dover Publications, 1934

(10) Robinson, A., and Laurmann, J.A., Wing Theory Cambridge, University Press, 1956

(11) Weber, J., "The Calculation of Pressure Distribution Over the Surface of Two Dimensional and Swept Wings with Symmetrical Aerofoil Sections", A.R.C. Technical Report, R&M No. 2918, July 1953

(12) Weber, J., "The Calculation of the Pressure Distribution on the Surface of Thick Cambered Wings and the Design of Wings with Given Pressure Distribution", A.R.C. Technical Report, R&M No. 3026, 1957

(13) Wendel, J.A.W.C., "Theoretical Analysis of Flapped Rudders", M.S. Thesis, Dept. of Naval Architecture and Marine Engineering, M.I.T., 1969

(14) Young, A.D., "The Aerodynamic Characteristics of Flaps" A.R.C. Technical Report, R&M No. 2622, 1953

(15) Stromberg-Carlson, "Datagraphix 4020 Computer Recorder" Programmer's Reference Manual

Thesis
C364 Champlain
Analysis of flapped
rudder gap effects.
127245